Stereotypic Neutralizing V_H Clonotypes Against SARS-CoV-2 RBD in COVID-19 Patients and the Healthy Population

Sang Il Kim[1,2†], Jinsung Noh[3†], Sujeong Kim[1,4], Younggeun Choi[1], Duck Kyun Yoo[1,2,4], Yonghee Lee[3], Hyunho Lee[3], Jongtak Jung[5], Chang Kyung Kang[5], Kyoung-Ho Song[5], Pyoeng Gyun Choe[5], Hong Bin Kim[5], Eu Suk Kim[5], Nam-Joong Kim[5], Moon-Woo Seong[6], Wan Beom Park[5], Myoung-don Oh[5], Sunghoon Kwon[3,7,8,9,10*], and Junho Chung[1,4,11*].

[1]Department of Biochemistry and Molecular Biology, Seoul National University College of Medicine, Seoul 03080, Korea.
[2]Ischemic/Hypoxic Disease Institute, Seoul National University Medical Research Center, Seoul 03080, Republic of Korea.
[3]Department of Electrical and Computer Engineering, Seoul National University, Seoul 08826, Republic of Korea.
[4]Department of Biomedical Science, Seoul National University College of Medicine, Seoul 03080, Republic of Korea.
[5]Department of Internal Medicine, Seoul National University College of Medicine, 03080 Seoul, Republic of Korea.
[6]Department of Laboratory Medicine, Seoul National University College of Medicine, 03080 Seoul, Republic of Korea.
[7]Interdisciplinary Program in Bioengineering, Seoul National University, Seoul, 08826, Republic of Korea.
[8]BK21+ Creative Research Engineer Development for IT, Seoul National University, Seoul, 08826, Republic of Korea.
[9]Biomedical Research Institute, Seoul National University Hospital, Seoul, 03080, Republic of Korea.
[10]Institutes of Entrepreneurial BioConvergence, Seoul National University, Seoul, 08826, Republic of Korea.
[11]Cancer Research Institute, Seoul National University College of Medicine, Seoul 03080, Korea.
*Correspondence to: skwon@snu.ac.kr (S.K.); jjhchung@snu.ac.kr (J.C.)
†These authors contributed equally to this work.

Abstract

In six of seven severe acute respiratory syndrome coronavirus 2 (SARS-CoV-2) patients, V_H clonotypes, encoded by either immunoglobin heavy variable (IGHV)3-53 or IGHV3-66 and immunoglobin heavy joining (IGHJ)6, were identified in IgG_1, IgA_1, and IgA_2 subtypes, with minimal mutations, and could be paired with diverse light chains, resulting in binding to the SARS-CoV-2 receptor-binding domain (RBD). Because most human antibodies against the RBD neutralized the virus by inhibiting host cell entry, we selected one of these clonotypes and demonstrated that it could potently inhibit viral replication. Interestingly, these V_H clonotypes pre-existed in six of 10 healthy individuals, predominantly as IgM isotypes, which could explain the expeditious and stereotypic development of these clonotypes among SARS-CoV-2 patients.

Main Text

Stereotypic neutralizing antibodies (nAbs) that are identified in convalescent patients can be valuable, providing critical information regarding the epitopes that should be targeted during the development of a vaccine [1,2]. Those antibodies with naïve sequences, little to no somatic mutations, and IgM or IgD isotypes are precious [3,4] because these characteristics effectively exclude the possibility that these nAbs evolved from pre-existing clonotypes that are reactive to similar viruses. This critical phenomenon is referred to as original antigenic sin (OAS), and predisposed antibody-dependent enhancement (ADE) enhancing the severity of viral infections, which can sometimes be fatal, as in the case of the dengue virus vaccine [5-8]. Several groups have identified nAbs for severe acute respiratory syndrome coronavirus 2 (SARS-CoV-2) [9-13], and one report has suggested the possibility that stereotypic nAbs may exist among convalescent patients [9]. However, stereotypic nAbs for SARS-CoV-2 have not

yet been identified. Here, we report stereotypic nAbs for SARS-CoV-2, which were identified by mapping nAbs onto deep immunoglobulin repertoires that were profiled from infected patients. One of these stereotypic nAbs was perfectly naïve and was encoded by immunoglobin heavy variable (IGHV)3-53/IGHV3-66 and immunoglobin heavy joining (IGHJ)6. Furthermore, we also found that these exact V_H clonotypes pre-exist in the majority of the healthy population, predominantly as an IgM isotype, which immediately provoked the hypothesis that individuals with this V_H clonotype may be able to rapidly evolve potent nAbs and experience favorable clinical features, similar to the human immunodeficiency virus (HIV)-1 response observed among individuals who acquire a unique V_H clonotype, featuring a very long heavy chain complementarity determining region (HCDR)3, following exposure to syphilis infection [14].

To obtain monoclonal nAbs against SARS-CoV-2, we collected blood samples from seven SARS-CoV-2-infected patients (patients A–G) and used them to generate human antibody libraries. Similar to SARS-CoV, SARS-CoV-2 also uses a spike (S) protein for receptor binding and membrane fusion [15]. This protein interacts with the cellular receptor angiotensin-converting enzyme II (ACE2) to gain entry into the host cell [16,17]. A previous report suggested that a human monoclonal antibody, which reacted with the receptor-binding domain (RBD), within the S1 region of the S protein, could hinder the initial interaction between the virus and the cell, effectively neutralizing SARS-CoV-2 [13]. We confirmed the reactivity of the sera derived from patients against recombinant SARS-CoV-2 S and RBD proteins. Patients A and E, who presented with extensive pneumonic infiltrates, also showed high plasma IgG levels against all recombinant SARS-CoV-2 nucleocapsid (NP), S, S1, S2, and RBD proteins, which could be detected 11, 17, and 45 days after symptom onset in Patient A and 23, 44, and 99 days after symptom onset in Patient E (Supplementary Table 1

and Supplementary Fig. 1). Notably, the sera samples from Middle East respiratory syndrome coronavirus (MERS-CoV) patients cross-reacted with the SARS-CoV-2 S protein, showing a higher titer against the S2 domain, and vice versa (Supplementary Fig. 1 and 2), suggesting the potential risk for ADE. We generated four human antibody libraries, utilizing a phage display system, based on the blood samples from Patient A, which were collected on days 17 and 45 (A_d17 and A_d45), and Patient E, which were collected on days 23 and 44 (E_d23 and E_d44). After biopanning, we successfully isolated 38 single-chain variable fragment (scFv) clones that were reactive against recombinant SARS-CoV-2 RBD in an enzyme immunoassay (Supplementary Fig. 3 and Supplementary Table 2). The half-maximal binding of these scFv-human kappa light chain fragment (hCκ) fusion proteins with the coated antigens occurred at concentrations ranging from 0.32 to 364 nM, which was compatible with the findings of previous reports that have described human monoclonal antibodies against SARS-CoV-2 RBD [10,13]. Then, we tested whether these antibody clones could inhibit the binding between recombinant SARS-CoV-2 S protein and Vero E6 cells expressing the ACE2 receptor. When incubated with 1.5×10^5 Vero E6 cells, the recombinant HIS-tagged SARS-CoV-2 S protein showed saturated binding at 200 nM, according to flow cytometry analysis, using a fluorescein isothiocyanate (FITC)-labeled anti-HIS antibody. For the analysis, recombinant S protein (200 nM) was mixed with scFv-hFc fusion proteins, at a final concentration of either 200 nM (equimolar) or 600 nM (molar ratio of 1:3). Eleven clones (A-1A1, A-1H4, A-1H12, A-2F1, A-2H4, E-2G3, E-3A12, E-3B1, E-3G9, E-3H31, and E-4D12) almost completely inhibited the binding between recombinant S protein and Vero E6 cells at 600 nM, and some showed potent inhibition activity, even at 200 nM (Supplementary Fig. 4). The neutralizing potency of these 11 clones for the inhibition of viral replication was tested using an *in vitro* assay. Vero cells, in a T-25 flask, were infected with SARS-CoV-2, at

a medium tissue culture infectious dose ($TCID_{50}$) of 2,500 and in the presence of scFv-hCκ fusion proteins, at concentrations of 0.5, 5, or 50 μg/mL. Viral RNA concentrations in the culture supernatant were determined 0, 24, 48, and 72 hours after infection. Nine antibodies exhibited complete neutralizing activity, at 50 μg/mL (Supplementary Fig. 5), and two antibodies (A-1H4 and E-3G9) showed potent neutralization, even at 5 μg/mL (Supplementary Fig. 5).

We also performed deep profiling of the immunoglobulin (IG) repertoire in three chronological blood samples each from patients A and E and two chronological samples from each of the other five patients. Then, we searched for nAb clonotypes that possessed identical VJ combinations and perfectly matched HCDR3 sequences, at the amino acid level among the immunoglobulin heavy chain (IGH) repertoires of Patients A and E. One and five nAb clonotypes were successfully identified in Patients A and E, respectively (Fig. 1a). Notably, three nAbs (A-2F1, E-3A12, and E-3B1) were encoded by IGHV3-53/IGHV3-66 and IGHJ6 (Fig. 1a). These two V_H genes, IGHV3-53*01 and IGHV3-66*01, are identical at the amino acid level, except for the H12 residue (isoleucine in IGHV3-53 and valine in IGHV3-66), and only five nucleotide differences exist between their sequences. Furthermore, four clonotypes were IgG_1, and two clonotypes class-switched to IgA_1 and IgA_2 when examined 44 days after symptom onset (Fig. 1a). These clonotypes had a very low frequency of somatic mutations (1.03% ± 0.51%), which was compatible with findings regarding other nAbs in previous reports [9,10]. Then, we collected all V_H sequences from the seven patients and searched the clonotypes of 11 nAbs that were encoded by the same V_H and J_H genes and showed 66.6% or higher identity in the HCDR3 sequence, at the amino acid level (Supplementary Fig. 6). Interestingly, clonotypes that were highly homologous to the E-3B1 nAb were found among six of seven patients, with a total of 55 sequences among the isotypes IgG_1 (Patient A, B, D,

E, F, and G), IgA_1 (Patient E and G), and IgA_2 (Patient E) (Supplementary Table 3). These clonotypes shared nearly identical V_H sequences (92.78% ±1.40% identity at the amino acid level), with E-3B1 displaying an extremely low frequency of somatic mutations (0.77% ± 0.93%). Among these 55 clonotypes, 22 unique HCDR3s were identified, at the amino acid level, and eight unique HCDR3s existed in more than one patient. To test the reactivity of clonotypes homologous to E-3B1 against the SARS-CoV-2 S protein, we arbitrarily sampled 12 IGH clonotypes (Fig. 1b), containing five different HCDR3s, from the IGH repertoires of six patients. The genes encoding these IGH clonotypes were chemically synthesized and used to construct scFv genes, using the V_λ gene from the E-3B1 clone. Then, the reactivities of these scFv clones were tested in an enzyme immunoassay. Three clones (E-12, A-32, and B-33) reacted against the recombinant S and RBD proteins (Fig. 1b). Then, scFv libraries were constructed, using the A-11, A-31, E-34, A,B,G-42, G-44, D-51, F-53, E-52, and A-54 genes, and the V_κ/V_λ genes were amplified from Patients A, E, and G. Consequently, we confirmed that all 12 IGH clonotypes were reactive against both recombinant S and RBD proteins when paired with eight different V_κ and V_λ genes (Fig. 1b,c). Moreover, all seven patients possessed these V_κ/V_λ clonotypes with identical VJ gene usage and perfectly matched LCDR3 amino acid sequences (Supplementary Fig. 7). In particular, IGLV2-14/IGLJ3, IGLV3-19/IGLJ2, and IGLV3-21/IGLJ2 were frequently used across all seven patients (Supplementary Fig. 8 and 9). Because E-3B1 effectively inhibited the replication of SARS-CoV-2 (Fig. 1d), these 55 clonotypes are likely to neutralize the virus when paired with an optimal light chain.

Among these IGH clonotypes, A,B,G-42 was quite unique, presenting no somatic mutations and containing an HCDR3 (DLYYYGMDV) formed by the simple joining of IGHV3-53 and IGHJ6. This naïve V_H sequence existed in the IGH repertoire of three patients (A, B, and G),

as IgG_1, IgG_1, or IgG_1 and IgA_1 subtypes, respectively (Table 1). More interestingly, the IGH clonotypes encoded by IGHV3-53/IGHV3-66 and IGHJ6 that possessed an HCDR3 (DLYYYGMDV) with zero to one somatic mutation residues could be identified within the IGH repertoire of six of 10 healthy individuals, predominantly as an IgM isotype (Table 1), based on publicly available IGH repertoires [18]. The A,B,G-42 clonotype showed light chain plasticity and paired with five V_κ /V_λ genes to achieve RBD binding. In particular, the V_κ gene (2J6H) accumulated only five somatic mutations (1.4% divergence). None of the 12 clones, including A,B,G-42, reacted against the recombinant RBD proteins from either SARS-CoV or MERS-CoV (Supplementary Fig. 10). In our prior experiment, none of the 37 identified MERS-RBD-binding human monoclonal antibodies, from two patients, were encoded by IGHV3-53/IGHV3-66 and IGHJ6 (Supplementary Table 4) [19]. Therefore, the presence of these stereotypic-naïve IGH clonotypes in the healthy population, and their light chain plasticity to achieve SARS-CoV-2 RBD binding, may be unique to SARS-CoV-2, which might provide a rapid and effective humoral response to the virus among patients who express these clonotypes. These findings provide the majority of the population possess germline-precursor B cells, encoded by IGHV3-53/IGHV3-66 and IGHJ6, which can actively initiate virus neutralization upon SARS-CoV-2 infection.

To further elucidate the preferential use of IGHV3-53/IGHV3-66 and IGHJ6 genes during the generation of SARS-CoV-2 RBD-binding antibodies, we extracted 252 predicted RBD-binding clones from our biopanning data (See Methods). We previously showed that antibody clones with binding properties can be predicted by employing next-generation sequencing (NGS) technology and analyzing the enrichment patterns of biopanned clones [20,21]. Although the IGHJ4 gene was more prominent in the IGH repertoires of the seven patients, similar to healthy human samples [18,22], the predicted RBD-binding clones primarily used the IGHJ6

gene (Fig. 1e). Furthermore, the predicted RBD-binding clones showed the dominant usage of IGHV3-53/IGHJ6 and IGHV3-66/IGHJ6 pairs, which was not observed in the whole IGH repertoires of patients (Fig. 1f).

Naïve B cells typically undergo somatic hypermutations, clonal selection, and class-switching following antigen exposure. We examined the chronological events that occurred in all IGH clonotypes identified in patients and those that were reactive against the SARS-CoV-2 RBD. We categorized RBD-reactive clones into three groups: neutralizing antibodies (neutralize), binding-confirmed antibodies (bind), and binding-predicted antibodies (predicted). In all three groups, these IGH clonotypes appeared and disappeared along the disease course and showed a low frequency of somatic mutations (Fig. 2c,d) and rapid class-switching, especially to IgG_1, IgA_1, and IgA_2. In the entire IGH repertoire of the patients, naïve-derived IGH clonotypes with minimal somatic mutations ($< 2.695\% \pm 0.700\%$) showed increased IgG_3 and IgG_1 subtypes, and the proportion of IgG_1 subtype was dramatically increased for a period (Fig. 2a,b and Supplementary Fig. 11). Furthermore, these naïve-derived IGH clonotypes were detected as IgA_1 and IgG_2 subtypes in patients A and E, as minor populations (Fig. 2a,b), and as the IgA_2 subtype in Patient E (Fig. 2b). To summarize, RBD-reactive IGH clonotypes rapidly emerged and underwent class-switching, to IgG_1, IgA_1, and IgA_2, without experiencing many somatic mutations. However, this dramatic temporal surge of naïve IGH clonotypes, with rapid class-switching, occurred across the entire IGH repertoire of patients and was not confined to those reactive to the SARS-CoV-2 RBD.

Because several mutations within the RBD have been identified along the course of the SARS-CoV-2 pandemic, worldwide [23], we examined the probability of emerging escape mutants from the IGH repertoire induced by the wild-type virus infection. Our E-3B1, A-1H4, A-2F1, A-2H4, and E-3G9 nAbs successfully bound to recombinant mutant RBD

proteins (V341I, F342L, N354D/D364Y, V367F, A435S, W436R, G476S, and V483A) in a dose-dependent manner, with compatible reactivity against recombinant wild-type RBD protein (Supplementary Fig. 12). Therefore, the human IGH immune repertoire may provide effective protection against most current SARS-CoV-2 mutants.

In response to SARS-CoV-2 infection, most human IGH repertoires efficiently generated clonotypes encoded by IGHV3-53/IGHV3-66 and IGHJ6, which could be paired with diverse light chains, for both RBD binding and virus neutralization, with few to no somatic mutations. These clonotypes underwent swift class-switching to IgG_1, IgA_1, and even IgA_2 subtypes. The expeditious development of these IGH clonotypes would be possible because the naïve-stereotypic IGHV3-53/IGHV3-66 and IGHJ6 clonotypes pre-exist in the majority of the healthy population, predominantly as an IgM isotype. In line with our findings, several groups have previously reported potent human nAbs, composed of either IGHV3-53 or IGHV3-66 and IGHJ6 genes, using single B cell sequencing technology [9-13]. Furthermore, the crystal structures of two IHGV3-53 neutralizing antibodies were determined which showed that two key motifs within HCDR1 and HCDR2 encoded in the IGHV3-53 germline are making contact with RBD [24]. Therefore, the preferential use of IGHV3-53/IGHV3-66 and IGHJ6 in the development of nAbs to SARS-CoV-2 appeared prominent. From these observations, we hypothesize that the existence of this unique, naïve IGH clonotype would provide near-immediate protection to some people exposed to SARS-CoV-2, and a very favorable clinical course, unlike SARS-CoV or MERS-CoV. In addition, the chronological follow-up of IGH clonotypes, encoded by the IGHV3-53/IGHV3-66 and IGHJ6 genes, along with their class-switching events, would be valuable for the development of a safe and effective vaccine.

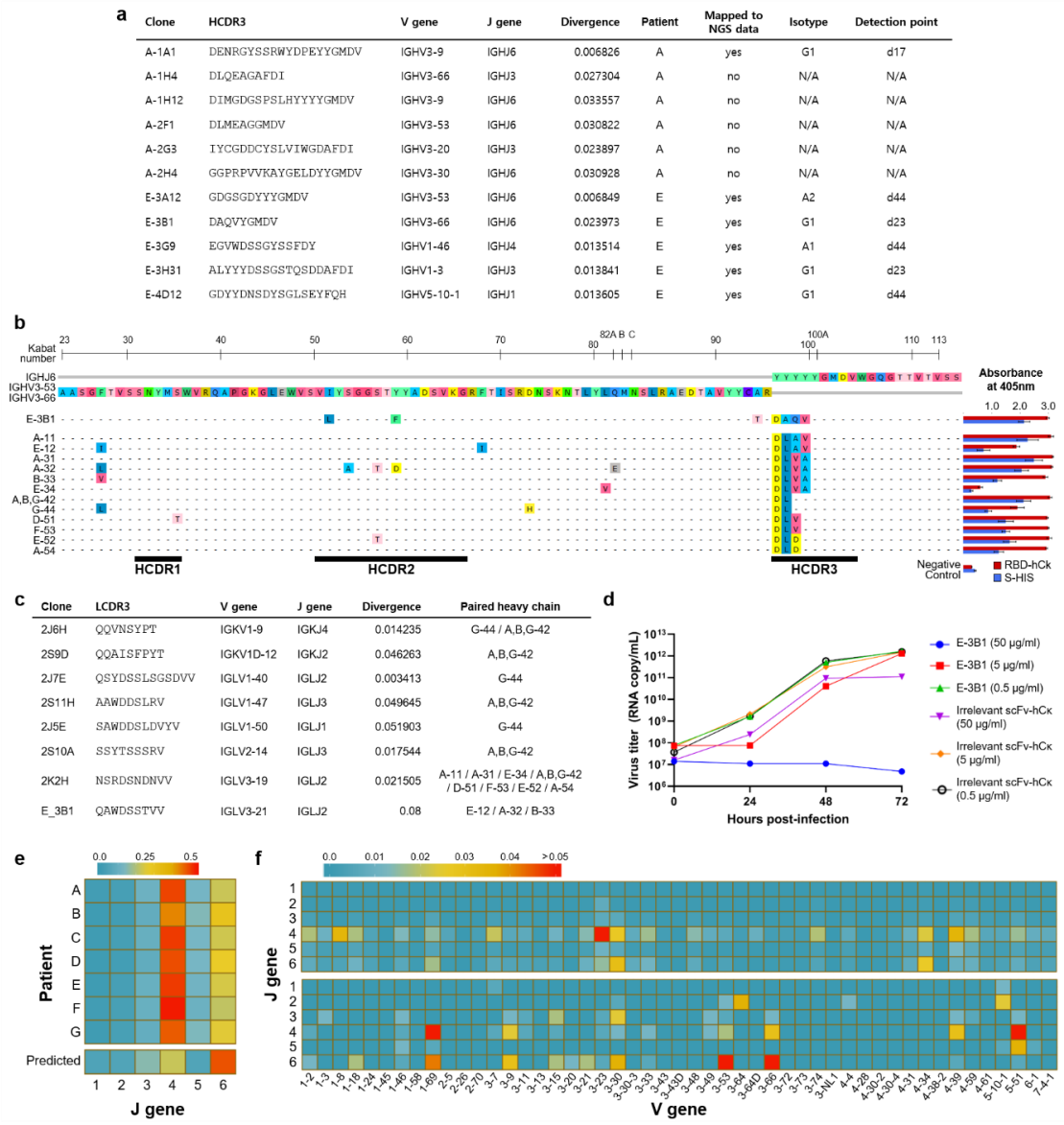

Clone	HCDR3	V gene	J gene	Divergence	Patient	Mapped to NGS data	Isotype	Detection point
A-1A1	DENRGYSSRWYDPEYYGMDV	IGHV3-9	IGHJ6	0.006826	A	yes	G1	d17
A-1H4	DLQEAGAFDI	IGHV3-66	IGHJ3	0.027304	A	no	N/A	N/A
A-1H12	DIMGDGSPSLHYYYYGMDV	IGHV3-9	IGHJ6	0.033557	A	no	N/A	N/A
A-2F1	DLMEAGGMDV	IGHV3-53	IGHJ6	0.030822	A	no	N/A	N/A
A-2G3	IYCGDDCYSLVIWGDAFDI	IGHV3-20	IGHJ3	0.023897	A	no	N/A	N/A
A-2H4	GGPRPVVKAYGELDYYGMDV	IGHV3-30	IGHJ6	0.030928	A	no	N/A	N/A
E-3A12	GDGSGDYYYGMDV	IGHV3-53	IGHJ6	0.006849	E	yes	A2	d44
E-3B1	DAQVYGMDV	IGHV3-66	IGHJ6	0.023973	E	yes	G1	d23
E-3G9	EGVWDSSGYSSFDY	IGHV1-46	IGHJ4	0.013514	E	yes	A1	d44
E-3H31	ALYYYDSSGSTQSDDAFDI	IGHV1-3	IGHJ3	0.013841	E	yes	G1	d23
E-4D12	GDYYDNSDYSGLSEYFQH	IGHV5-10-1	IGHJ1	0.013605	E	yes	G1	d44

Clone	LCDR3	V gene	J gene	Divergence	Paired heavy chain
2J6H	QQVNSYPT	IGKV1-9	IGKJ4	0.014235	G-44 / A,B,G-42
2S9D	QQAISFPYT	IGKV1D-12	IGKJ2	0.046263	A,B,G-42
2J7E	QSYDSSLSGSDVV	IGLV1-40	IGLJ2	0.003413	G-44
2S11H	AAWDDSLRV	IGLV1-47	IGLJ3	0.049645	A,B,G-42
2J5E	SAWDDSLDVYV	IGLV1-50	IGLJ1	0.051903	G-44
2S10A	SSYTSSSRV	IGLV2-14	IGLJ3	0.017544	A,B,G-42
2K2H	NSRDSNDNVV	IGLV3-19	IGLJ2	0.021505	A-11 / A-31 / E-34 / A,B,G-42 / D-51 / F-53 / E-52 / A-54
E_3B1	QAWDSSTVV	IGLV3-21	IGLJ2	0.08	E-12 / A-32 / B-33

Fig. 1 | Characteristics of nAbs, derived from patients A and E, stereotypic IGH clonotypes that are highly homologous to E-3B1, and the predicted RBD-binding clones that were enriched through biopanning. Stereotypic nAb V_H clonotypes against the SARS-CoV-2 RBD, encoded by IGHV3-53/3-66 and IGHJ6, were found in six of seven patients. **a,** Characteristics of nAbs discovered in patients A and E. **b,** IGH clonotypes that are highly homologous to E-3B1 and reactive against recombinant SARS-CoV-2 S and RBD proteins. The right column shows the results of the phage ELISA. All experiments were performed in quadruplicate, and the data are presented as the mean ± SD. **c,** List of diverse IGL clonotypes that can be paired with the IGH clonotypes from **b** to achieve reactivity. **d,** Measurement of viral RNA in the culture supernatant of Vero cells after SARS-CoV-2 infection **e,** J and **f,** VJ gene usage in the IGH repertoire of patients (upper) and the binding-predicted IGH clones (bottom). For the VJ gene usage heatmap, the frequency values for the IGH repertoire of all seven patients were averaged and are displayed (upper) along with those of the predicted RBD-binding IGH clones (bottom). N/A: not applicable

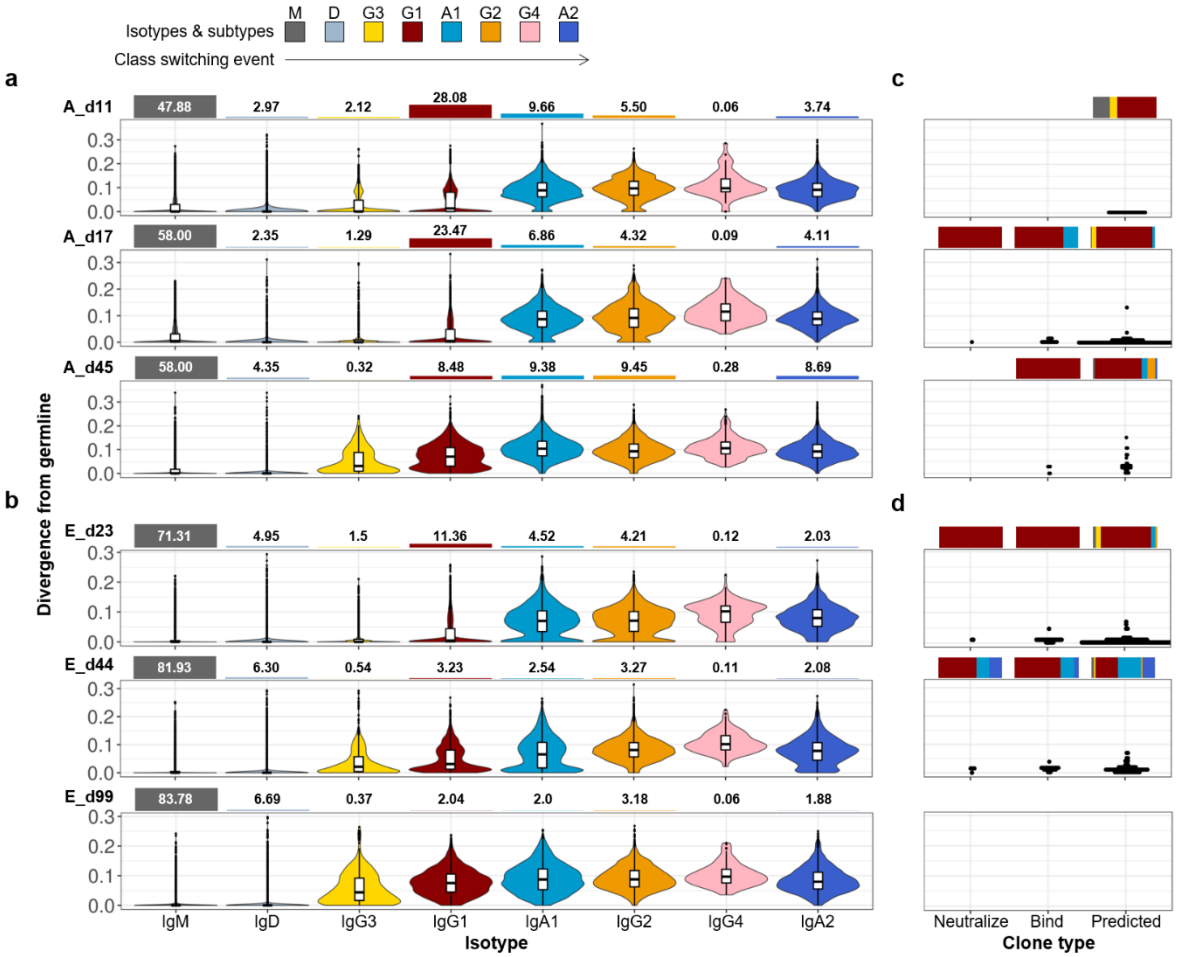

Fig. 2 | Deep profiling of the IGH repertoires of patients A and E. RBD-reactive IGH clonotypes rapidly undergo class-switching events to IgG_1, IgA_1, and IgA_2, with few somatic mutations. **(a,b)** IGH repertoires of **a,** Patient A and **b,** Patient E were analyzed 11, 17, and 45 (A_d11, A_d17, A_d45) days and 23, 44, and 99 (E_d23, E_d44, E_d99) days after symptom onset, respectively. IGH repertoires were examined according to divergence from the germline and the isotype composition of the sequences. Values for divergence from the germline were calculated separately for each isotype and are presented as violin plots, ordered by the class-switch event. The bar graphs on the top of the violin plots represent the proportion of each isotype in the repertoire. (**c,d)** Mapping of three types of RBD-binding IGH sequences (neutralize, bind, and predicted), derived from either **c,** Patient A or **d,** Patient E, against the corresponding IGH repertoire. The positions of the RBD-binding IGH sequences in the divergence value were annotated as dot plots, on the same scale used for **a** and **b**. Bar graphs on the top of the dot plots indicate the isotype compositions of the sequences in the repertoire.

Table1. The stereotypic V_H clonotypes against SARS-CoV-2 RBD in the healthy population and patients

Healthy population						
sample	**V gene**	**J gene**	**CDR3 AA**	**Divergence**	**Isotype**	**Occurrence**
326650	IGHV3-53 / 3-66	IGHJ6	DLYYYGMDV	0.007 ± 0.003	M (100%)	12
326713	IGHV3-53 / 3-66	IGHJ6	DLYYYGMDV	0.005 ± 0.010	M (92.3%), G (7.7%)	13
326780	IGHV3-53 / 3-66	IGHJ6	DLYYYGMDV	0.014 ± 0.010	M (97.4%), G (2.6%)	38
326797	IGHV3-53	IGHJ6	DLYYYGMDV	0.004	M (100%)	1
327059	IGHV3-53 / 3-66	IGHJ6	DLYYYGMDV	0.003 ± 0.005	M (100%)	8
D103	IGHV3-53	IGHJ6	DLYYYGMDV	0.008 ± 0.020	M (100%)	9
326650	IGHV3-53 / 3-66	IGHJ6	DLDYYGMDV	0.006 ± 0.002	M (75%), G (25%)	4
326713	IGHV3-53 / 3-66	IGHJ6	DLDYYGMDV	0.012 ± 0.018	M (100%)	4
326797	IGHV3-66	IGHJ6	DLDYYGMDV	0.055	M (100%)	1
327059	IGHV3-53 / 3-66	IGHJ6	DLDYYGMDV	0.001 ± 0.002	M (100%)	4
D103	IGHV3-53	IGHJ6	DLDYYGMDV	0.053	M (100%)	1
326713	IGHV3-53 / 3-66	IGHJ6	DLVAYGMDV	0.008 ± 0.011	M (100%)	2
326713	IGHV3-53	IGHJ6	DLVYYGDMV	0.001 ± 0.002	M (100%)	3
326797	IGHV3-53	IGHJ6	DLVYYGMDV	0.089 ± 0.008	M (100%)	2
SARS-CoV-2-infected patients						
sample	**V gene**	**J gene**	**CDR3 AA**	**Divergence**	**Isotype**	**Occurrence**
A	IGHV3-53	IGHJ6	DLYYYGMDV	0.002 ± 0.004	M (5.1%), G1 (94.9%)	59
B	IGHV3-53	IGHJ6	DLYYYGMDV	0.000 ± 0.000	M (33.3%), G1 (66.7%)	3
G	IGHV3-53 / 3-66	IGHJ6	DLYYYGMDV	0.005 ± 0.003	G1 (84.6%), A1 (15.4%)	14
A	IGHV3-53	IGHJ6	DLAVYGMDV	0.004 ± 0.000	G1 (100%)	2
E	IGHV3-66	IGHJ6	DLAVYGMDV	0.018 ± 0.000	G1 (100%)	6
A	IGHV3-53	IGHJ6	DLDYYGMDV	0.000 ± 0.000	G1 (100%)	3
E	IGHV3-53	IGHJ6	DLDYYGMDV	0.004 ± 0.000	A1 (100%)	4
A	IGHV3-53	IGHJ6	DLVAYGMDV	0.008 ± 0.017	G1 (100%)	14
B	IGHV3-53	IGHJ6	DLVAYGMDV	0.009	G1 (100%)	1
E	IGHV3-53	IGHJ6	DLVAYGMDV	0.005 ± 0.002	G1 (100%)	6
D	IGHV3-53	IGHJ6	DLVYYGMDV	0.004	G1 (100%)	1
E	IGHV3-53	IGHJ6	DLVYYGMDV	0.013	A1 (100%)	1

The healthy samples based on publicly available IGH repertoires or patient identification can be found in the sample column. Clonotypes were mapped according to identical VJ gene usage of IGHV3-53/IGHV3-66 and IGHJ6 and perfectly matched HCDR3 at the amino acid level. The read counts of the mapped sequences in the repertories of each samples were annotated in the occurrence column. For the clonotypes with multiple occurrences, mean and standard deviation of divergence were represented. The proportion of each isotypes were indicated for the all samples.

Methods

Human samples. Three chronological blood samples were drawn from Patients A and E. From Patients B, C, D, F, and G, two chronological samples were obtained. All patients were confirmed to be infected by SARS-CoV-2 by a positive reverse transcriptase-quantitative polymerase chain reaction (RT-qPCR) result, and sample collection was performed at Seoul National University Hospital. Peripheral blood mononuclear cells (PBMCs) and plasma were isolated using Lymphoprep (Stemcell Technologies, Vancouver, BC, Canada), according to the manufacturer's protocol. The PBMCs were subjected to total RNA isolation, using the TRI Reagent (Invitrogen, Carlsbad, CA, USA), according to the manufacturer's protocol. The study involving human sample collection was approved by the Institutional Ethics Review Board of Seoul National University Hospital (IRB approval number: 2004-230-1119).

Next-generation sequencing (NGS). Genes encoding V_H and part of the CH1 domain were amplified, using specific primers, as described previously [18,25]. All primers used are listed in Supplementary Table 8. Briefly, total RNA was used as a template to synthesize cDNA, using the Superscript IV First-Strand Synthesis System (Invitrogen), with specific primers targeting the constant region (CH1 domain) of each isotype (IgM, IgD, IgG, IgA, and IgE) [25], according to the manufacturer's protocol. Following cDNA synthesis, 1.8 volumes of SPRI beads (AmpureXP, Beckman Coulter, Brea, CA, USA) were used to purify cDNA, which was eluted in 40 µL water. The purified cDNA (18 µL) was subjected to second-strand synthesis in a 25-µL reaction volume, using V gene-specific primers [18] and KAPA Biosystems (KAPA HiFi HotStart, Roche, Basel, Switzerland). The PCR conditions were as follows: 95°C for 3 min, 98°C for 1 min, 55°C for 1 min, and 72°C for 5 min. Following the second-strand synthesis, double-strand DNA (dsDNA) was purified, using SPRI beads, as

described above. V_H genes were amplified using 15 µL eluted dsDNA and 2.5 pmol of the primers listed in Supplementary Supplementary Table 8, in a 50-µL total reaction volume (KAPA Biosystems), using the following thermal cycling program: 95°C for 3 min; 17 cycles of 98°C for 30 sec, 65°C for 30 sec, and 72°C for 1 min 10 sec; and 72°C for 5 min. The number of PCR cycles was increased, from 17 to 19, for samples from Patients B (d10 and 19), C (d6), E (d23), and G (d9 and 22). PCR products were purified using SPRI beads and eluted in 30 µL water. Genes encoding V_κ and V_λ were amplified using specific primers, as described previously [22,26]. Briefly, total RNA was used as a template to synthesize cDNA, using the Superscript IV First-Strand Synthesis System (Invitrogen), with specific primers targeting the constant region, which are listed in Supplementary Table 8, according to the manufacturer's protocol. Following cDNA synthesis, SPRI beads were used to purify cDNA, which was eluted in 40 µL water. Purified cDNA (18 µL) was used for the first amplification, in a 25-µL reaction volume, using VJ gene-specific primers, which are listed in Supplementary Table 8, and KAPA Biosystems. The PCR conditions were as follows: 95°C for 3 min, 4 cycles of 98°C for 1 min, 55°C for 1 min, and 72°C for 1 min; and 72°C for 10 min. Subsequently, DNA was purified using SPRI beads, and the V_κ and V_λ genes were amplified using 15 µL eluted dsDNA and 2.5 pmol of the primers listed in Supplementary Table 8, in a 50-µL total reaction volume (KAPA Biosystems). The PCR conditions were as follows: 95°C for 3 min; 17 cycles of 98°C for 30 sec, 65°C for 30 sec, and 72°C for 1 min 10 sec; and 72°C for 5 min. PCR products were purified using SPRI beads, as described above. For the amplification of V_H from each round of biopanning (rounds 0–4), gene fragments were amplified from phagemid DNA, using the primers listed in Supplementary Table 8. SPRI-purified sequencing libraries were quantified with a 4200 TapeStation System

(Agilent Technologies), using a D1000 ScreenTape Assay, before performing sequencing on an Illumina MiSeq Platform.

NGS data processing

Pre-processing of the NGS data for the IG repertoire. The raw NGS forward (R1) and reverse (R2) reads were merged by PEAR, v0.9.10, in default setting [27]. The merged reads were q-filtered using the condition q20p95, which results in 95% of the base-pairs in a read having Phread scores higher than 20. The location of the primers was recognized from the q-filtered reads while allowing one substitution or deletion (Supplementary Table 8). Then, primer regions that specifically bind to the molecules were trimmed in the reads, to eliminate the effects of primer synthesis errors. Based on the primer recognition results, unique molecular identifier (UMI) sequences were extracted, and the reads were clustered according to the UMI sequences. To eliminate the possibility that the same UMI sequences might be used for different read amplifications, the clustered reads were sub-clustered, according to the similarity of the reads (Five mismatches were allowed in each sub-cluster). The sub-clustered reads were aligned, using a multiple sequence alignment tool, Clustal Omega, v1.2.4, in default setting [28,29]. From the aligned reads, the frequency of each nucleotide was calculated, and a consensus sequence of each sub-cluster was defined using the frequency information. Then, the read count of the consensus sequence was re-defined as the number of UMI sub-clusters that belong to the consensus sequences.

Sequence annotation, functionality filtering, and throughput adjustment. Sequence annotation consisted of two parts, isotype annotation and VDJ annotation. For annotation, the consensus sequence was divided into two sections, a VDJ region and a constant region, in a

location-based manner. For isotype annotation, the extracted constant region was aligned with the IMGT (international immunogenetics information system) constant gene database [30]. Based on the alignment results, the isotypes of the consensus sequences were annotated. Then, the VDJ regions of the consensus sequences were annotated, using IgBLAST, v1.8.0 [31]. Among the annotation results, V/D/J genes (V/J genes for V_L), CDR1/2/3 sequences, and the number of mutations from the corresponding V genes were extracted, for further analysis. Divergence values were defined as the number of mutations identified in the aligned V gene, divided by the aligned length. Then, the non-functional consensus reads were defined using the following criteria and filtered-out: 1. sequence length shorter than 250 bp; 2. existence of stop-codon or frame-shift in the full amino acid sequence; 3. annotation failure in one or more of the CDR1/2/3 regions; and 4. isotype annotation failure. Then, the functional consensus reads were random-sampled, to adjust the throughput of the V_H data (Supplementary Table 5). Throughput adjustment was not conducted for V_L data (Supplementary Table 6).

Pre-processing of the biopanning NGS data. Pre-processing of the biopanning NGS data was performed as previously reported, except for the application of the q-filtering condition q20p95 instead of q20p100 [32].

Overlapping IGH repertoire construction. To investigate the shared IGH sequences among the patients, we defined the overlapping IGH repertoire of the patients. First, histograms for the nearest-neighbor distances of the HCDR3 amino acid sequences were calculated for the repertoire data. A hierarchical, distance-based analysis, which was reported previously [33], was applied to the HCDR3 amino acid sequences, to cluster the IGH sequences at a

functional level. The IGH sequences for all repertoire data could be approximated into a bimodal distribution, allowing the functionally similar IGH sequences to be extracted by capturing the first peak of the distribution (Supplementary Fig. 13). Threshold values for each data set were defined as the nearest-neighbor distance value of those points with a minimum frequency between the two peaks of the distribution. Then, the minimum value among all threshold values, 0.113871, was used to construct the overlapping IGH repertoire, which means that 11.3871% of mismatches in the CDR3 amino acid sequence were allowed in the overlapping IGH repertoire construction. To construct the overlapping IGH repertoire, the repertoire data sets of all patients were merged into one data set. The IGH sequences in the merged data set were then clustered, using the following conditions: 1. the same V and J gene usage; and 2. mismatch smaller than 11.3871% among the CDR3 amino acid sequences. Subsequently, clusters containing IGH sequences from more than one patient were included in the overlapping IGH repertoire data set.

Extraction of binding-predicted clones. From each round of biopanning (rounds 0, 2, 3, and 4), the V_H genes were amplified and subjected to NGS analysis, using the MiSeq platform, as described previously [21]. Binding-predicted clones from biopanning were defined by employing frequency the values of the NGS data from four libraries, A_d17, A_d45, E_d23, and E_d44, at each round of biopanning. The enrichment of clones primarily occurred during the second round of biopanning, based on the input/output virus titer values for each round of biopanning and the frequencies of the clones in the NGS data (Supplementary Fig. 14). Then, the frequency information in the NGS data sets for biopanning rounds 0, 2, 3, and 4 was subject to principal component analysis (PCA), for dimension reduction. Accordingly, principal component (PC)1 and PC2, which represented clone enrichment and clone

depletion, respectively, were extracted. In the biopanning data, PC1 was primarily composed of the frequencies in rounds 2, 3, and 4, whereas PC2 was primarily composed of the frequency in round 0 (Supplementary Fig. 15). Thus, we defined PC1-major clones as the predicted clones, by setting constant threshold values on the PC1 value and the ratio between PC1 and PC2 (Supplementary Table 7). Subsequently, 94.74% of the RBD-binding clones were successfully mapped to the predicted clones (Supplementary Fig. 15).

Construction of a human scFv phage-display library and V_L shuffled libraries. For the V_H gene, the cDNA prepared for the NGS analysis was used. For the V_K and V_λ genes, total RNA was used to synthesize cDNA, using the Superscript IV First-Strand Synthesis System (Invitrogen), with oligo(dT) primers, according to the manufacturer's instructions. Then, the genes encoding V_K/V_λ and V_H were amplified, from the oligo(dT)-synthesized cDNA and the cDNA prepared for NGS analysis, respectively, using the primers listed in Supplementary Table 8 and KAPA Biosystems. The PCR conditions were as follows: preliminary denaturation at 95°C for 3 min; 4 cycles of 98°C for 1 min, 55°C for 1 min, and 72°C for 1 min; and 72°C for 10 min. Subsequently, DNA was purified using SPRI beads, as described above. The purified DNA was amplified using the primers listed in Supplementary Table 8 and KAPA Biosystems. The PCR conditions were as follows: preliminary denaturation, at 95°C for 3 min; 25 cycles of 98°C for 30 sec, 58°C for 30 sec, and 72°C for 90 sec; and 72°C for 10 min. Then, the V_H and V_K/V_λ fragments were subjected to electrophoresis, on a 1% agarose gel, and purified, using a QIAquick Gel Extraction Kit (Qiagen Inc., Valencia, CA, USA), according to the manufacturer's instructions. The purified V_H and V_K/V_λ fragments were mixed, at equal ratios at 50 ng, and subjected to overlap extension, to generate scFv genes, using the primers listed in Supplementary Table 8 and KAPA Biosystems. The PCR

conditions were as follows: preliminary denaturation, at 94°C for 5 min; 25 cycles of 98°C for 15 sec, 56°C for 15 sec, and 72°C for 2 min; and 72°C for 10 min. The amplified scFv fragment was purified and cloned into a phagemid vector, as described previously [34].

For the construction of V_K/V_λ shuffled libraries, gBlocks Gene Fragments (Integrated DNA Technologies, Coralville, IA, USA), encoding A-11, E-12, A-31, A-32, B-33, E-34, A,B,G-42, G-44, D-51, F-53, E-52, and A-54, were synthesized. Synthesized V_H and the V_K/V_λ genes from Patients A, E, and G were used to synthesize the scFv libraries using PCR, as described previously [34]. Then, the amplified scFv fragments were purified and cloned into the phagemid vector, as described above.

Biopanning. A phage display of the human scFv libraries was subjected to four rounds of biopanning against the recombinant SARS-CoV-2 S and RBD proteins (Sino Biological Inc., Beijing, China), fused to mFc or hCκ, as described previously [35]. Briefly, 3 μg of the recombinant SARS-CoV-2 RBD protein was conjugated to 1.0×10^7 magnetic beads (Dynabeads M-270 epoxy, Invitrogen) and incubated with the scFv phage-display libraries (approximately 10^{12} phages), for 2 h at 37°C. During the first round of biopanning, the beads were washed once with 500 μL 0.05% (v/v) Tween-20 (Sigma-Aldrich, St. Louis, MO, USA) in phosphate-buffered saline (PBST). For the other rounds of biopanning, 1.5 μg recombinant SARS-CoV-2 RBD protein was conjugated to 5.0×10^6 magnetic beads, and the number of washes was increased to three. After each round of biopanning, the bound phages were eluted and rescued, as described previously [35].

Phage ELISA. To select SARS-CoV-2 S reactive clones, phage enzyme-linked immunosorbent assay (ELISA) was performed, using recombinant S and RBD protein-coated

microtiter plates, as described previously [36]. Reactive scFv clones were subjected to Sanger sequencing (Cosmogenetech, Seoul, Republic of Korea), to determine their nucleotide sequences.

Expression of recombinant proteins. A human, codon-optimized, SARS-CoV-2 RBD (YP_009724390.1, amino acids 306–543) gene was synthesized (Integrated DNA Technologies). Using a synthesized wild-type RBD gene as a template, RBD mutants (V341I, F342L, N354D, N354D/D364Y, V367F, R408I, A435S, W436R, G476S, and V483A) were generated through two-step PCR, using the primers listed in Supplementary Table 8. The genes encoding wild-type or mutant SARS-CoV-2 RBD were cloned into a modified mammalian expression vector, containing the hCκ gene [35], and transfected into Expi293F (Invitrogen) cells. The fusion proteins were purified by affinity chromatography, using KappaSelect Columns (GE Healthcare, Chicago, IL, USA), as described previously [37]. Due to low expression yields, two RBD mutants (N354D/D364Y, W436R) were excluded from further studies.

The genes encoding the selected scFv clones were cloned into a modified mammalian expression vector, containing the hIgG$_1$ Fc regions (hFc) or hCκ at the C-terminus [35,38], before being transfected and purified by affinity chromatography, as described above.

ELISA. First, 100 ng of each recombinant SARS-CoV-2 S (Sino Biological Inc.), S1 (Sino Biological Inc.), S2 (Sino Biological Inc.), NP (Sino Biological Inc.), RBD, RBD mutants, SARS-CoV RBD (Sino Biological Inc.), MERS-CoV S (Sino Biological Inc.), RBD (Sino Biological Inc.), S2 (Sino Biological Inc.) proteins were added to microtiter plates (Costar), in coating buffer (0.1 M sodium bicarbonate, pH 8.6). After incubation at 4°C, overnight, and

blocking with 3% bovine serum albumin (BSA) in PBS, for 1 h at 37°C, serially diluted plasma (5-fold, 6 dilutions, starting from 1:100) or scFv-hFc (5-fold, 12 dilutions, starting from 1,000 or 500 nM) in blocking buffer was added to individual wells and incubated for 1, h at 37°C. Then, the plates were washed three times with 0.05% PBST. Horseradish peroxidase (HRP)-conjugated rabbit anti-human IgG antibody (Invitrogen) or anti-human Ig kappa light chain antibody (Millipore, Temecula, CA, USA), in blocking buffer (1:5,000), was added into wells and incubated for 1 h at 37°C. After washing three times with PBST, 2,2′-azino-bis-3-ethylbenzothiazoline-6-sulfonic (ThermoFisher Scientific Inc., Waltham, MA, USA) or 3,3′,5,5′-Tetramethylbenzidine liquid substrate system (ThermoFisher Scientific Inc.) was added to the wells. Absorbance was measured at 405 nm or 650 nm, using a microplate spectrophotometer (Multiskan GO; Thermo Scientific).

Flow cytometry. The recombinant SARS-CoV-2 S protein (200 nM), fused with a polyhistidine tag at the C-terminus (Sino Biological Inc.), was incubated with scFv-hFc fusion proteins at a final concentration of either 200 nM (equimolar) or 600 nM (morlar ratio of 1:3), in 50 μL of 1% (w/v) BSA in PBS, containing 0.02% (w/v) sodium azide (FACS buffer), at 37°C for 1 h. Irrelevant scFv-hFc or scFv-hCκ fusion proteins were used as negative controls. Vero E6 cells ($ACE2^+$) were seeded into v-bottom 96-well plates (Corning, Corning, NY, USA), at a density of 1.5×10^5 cells per well. Then, the mixture was added to each well and incubated, at 37°C for 1 h. After washing three times with FACS buffer, FITC-labeled rabbit anti-HIS Ab (Abcam, Cambridge, UK) was incubated, at 37°C for 1 h. Then, the cells were washed three times with FACS buffer, resuspended in 150 μL of PBS, and subjected to analysis by flow cytometry, using a FACS Canto II instrument (BD Bioscience, San Jose, CA, USA). For each sample, 10,000 cells were assessed.

Microneutralization assay. The virus (BetaCoV/Korea/SNU01/2020, accession number MT039890) was isolated at the Seoul National University Hospital and propagated in Vero cells (ATCC CCL-81), using Dulbecco's Modified Eagle's Medium (DMEM, Welgene, Gyeongsan, Republic of Korea) supplemented with 2% fetal bovine serum (Gibco) [39]. The cells were grown in T-25 flasks, (ThermoFisher Scientific Inc.), inoculated with SARS-CoV-2, and incubated at 37°C, in a 5% CO_2 environment. Then, 3 days after inoculation, the viruses were harvested and stored at -80°C. The virus titer was determined via a $TCID_{50}$ assay [40].

Vero cells were seeded in T-25 flasks and grown for 24 h, at 37°C, in a 5% CO_2 environment, to ensure 80% confluency on the day of inoculation. The recombinant scFv-hCκ fusion proteins (0.5, 5, or 50 μg/mL) were mixed with 2,500 $TCID_{50}$ of SARS-CoV-2, and the mixture was incubated for 2 h, at 37°C. Then, the mixture (1 mL) was added to the Vero cells and incubated for 1 h, at 37°C, in a 5% CO_2 environment. After incubation for 1 h, 6 mL of complete media was added to the flasks and incubated, at 37°C, in a 5% CO_2 environment. After 0, 24, 48, and 72 h of infection, the culture supernatant was collected, to measure the virus titers. RNA was extracted, using the MagNA Pure 96 DNA and Viral NA small volume kit (Roche, Germany), according to the manufacturer's instructions. Viral RNA was detected using the PowerChek 2019-nCoV Real-time PCR Kit (Kogene Biotech, Seoul, Republic of Korea), for the amplification of the E gene, and quantified according to a standard curve, which was constructed using *in vitro* transcribed RNA, provided by the European Virus Archive (https://www.european-virus-archive.com).

Data and materials availability: Raw sequencing data will be submitted shortly. Computer codes and processed data will be deposited on Github. All other data that supporting the findings of this study are available from the corresponding author on reasonable request.

Acknowledgments: The authors thank Su Jin Choi for technical support. This research was funded by the National Research Foundation of Korea [NRF-2016M3A9B6918973] and the Ministry of Science and ICT(MSIT) of the Republic of Korea and the National Research Foundation of Korea [NRF-2020R1A3B3079653]. This research was supported by the Global Research Development Center Program, through the NRF, funded by the MSIT [2015K1A4A3047345]. This work was supported by the Brain Korea 21 Plus Project in 2020.

Author contributions: SangIl K. designed and conducted the experiments, performed analysis, interpreted experimental results, and wrote the paper. J.N. performed the bioinformatic analysis, visualized and interpreted results, and wrote the paper. Sujeong K. conducted experiments, performed analyses, and interpreted experimental results. Y.C., D.Y., and M.S. conducted the experiments. Y.L. and H.L. performed the bioinformatic analysis. J.J., C.K., K.S., P.C., H.K., E.K., and N.K. contributed to patient recruitment. W.P. conceived the study, designed and conducted experiments, and interpreted experimental results. M.O. conceived the study. S.K. conceived the study and designed and supervised the bioinformatics analysis. J.C. conceived the study, designed and supervised the experiments, interpreted all results, and wrote the paper.

Competing interests: The authors declare no competing interests.

References

1 Ehrhardt, S. A. *et al.* Polyclonal and convergent antibody response to Ebola virus vaccine rVSV-ZEBOV. *Nat Med* **25**, 1589-1600, doi:10.1038/s41591-019-0602-4 (2019).

2 Setliff, I. *et al.* Multi-Donor Longitudinal Antibody Repertoire Sequencing Reveals the Existence of Public Antibody Clonotypes in HIV-1 Infection. *Cell Host Microbe* **23**, 845-854 e846, doi:10.1016/j.chom.2018.05.001 (2018).

3 Jardine, J. G. *et al.* HIV-1 VACCINES. Priming a broadly neutralizing antibody response to HIV-1 using a germline-targeting immunogen. *Science* **349**, 156-161, doi:10.1126/science.aac5894 (2015).

4 Willis, J. R. *et al.* Long antibody HCDR3s from HIV-naive donors presented on a PG9 neutralizing antibody background mediate HIV neutralization. *Proc Natl Acad Sci U S A* **113**, 4446-4451, doi:10.1073/pnas.1518405113 (2016).

5 Eroshenko, N. *et al.* Implications of antibody-dependent enhancement of infection for SARS-CoV-2 countermeasures. *Nat Biotechnol*, doi:10.1038/s41587-020-0577-1 (2020).

6 Iwasaki, A. & Yang, Y. The potential danger of suboptimal antibody responses in COVID-19. *Nat Rev Immunol*, doi:10.1038/s41577-020-0321-6 (2020).

7 Smatti, M. K., Al Thani, A. A. & Yassine, H. M. Viral-Induced Enhanced Disease Illness. *Front Microbiol* **9**, 2991, doi:10.3389/fmicb.2018.02991 (2018).

8 Zhang, A., Stacey, H. D., Mullarkey, C. E. & Miller, M. S. Original Antigenic Sin: How First Exposure Shapes Lifelong Anti-Influenza Virus Immune Responses. *J Immunol* **202**, 335-340, doi:10.4049/jimmunol.1801149 (2019).

9 Cao, Y. *et al.* Potent neutralizing antibodies against SARS-CoV-2 identified by high-throughput single-cell sequencing of convalescent patients' B cells. *Cell*, doi:10.1016/j.cell.2020.05.025 (2020).

10 Ju, B. *et al.* Human neutralizing antibodies elicited by SARS-CoV-2 infection. *Nature*, doi:10.1038/s41586-020-2380-z (2020).

11 Rogers, T. F. *et al.* Rapid isolation of potent SARS-CoV-2 neutralizing antibodies and protection in a small animal model. *bioRxiv*, 2020.2005.2011.088674, doi:10.1101/2020.05.11.088674 (2020).

12 Shi, R. *et al.* A human neutralizing antibody targets the receptor binding site of SARS-CoV-2. *Nature*, doi:10.1038/s41586-020-2381-y (2020).

13 Wu, Y. *et al.* A noncompeting pair of human neutralizing antibodies block COVID-19 virus binding to its receptor ACE2. *Science*, doi:10.1126/science.abc2241 (2020).

14 Haynes, B. F. *et al.* Cardiolipin polyspecific autoreactivity in two broadly neutralizing HIV-1 antibodies. *Science* **308**, 1906-1908, doi:10.1126/science.1111781 (2005).

15 Wrapp, D. *et al.* Cryo-EM structure of the 2019-nCoV spike in the prefusion conformation. *Science* **367**, 1260-1263, doi:10.1126/science.abb2507 (2020).

16 Wang, Q. *et al.* Structural and Functional Basis of SARS-CoV-2 Entry by Using Human ACE2. *Cell* **181**, 894-904 e899, doi:10.1016/j.cell.2020.03.045 (2020).

17 Zhou, P. *et al.* A pneumonia outbreak associated with a new coronavirus of probable bat origin. *Nature* **579**, 270-273, doi:10.1038/s41586-020-2012-7 (2020).

18 Briney, B., Inderbitzin, A., Joyce, C. & Burton, D. R. Commonality despite exceptional diversity in the baseline human antibody repertoire. *Nature* **566**, 393-397, doi:10.1038/s41586-019-0879-y (2019).

19 Kim, S. I. *et al.* Generation of a Nebulizable CDR-Modified MERS-CoV Neutralizing Human Antibody. *Int J Mol Sci* **20**, doi:10.3390/ijms20205073 (2019).

20 Yang, W. *et al.* Next-generation sequencing enables the discovery of more diverse positive clones from a phage-displayed antibody library. *Exp Mol Med* **49**, e308, doi:10.1038/emm.2017.22 (2017).

21 Yoo, D. K. *et al.* Machine Learning-Guided Prediction of Antigen-Reactive In Silico Clonotypes Based on Changes in Clonal Abundance through Bio-Panning. *Biomolecules* **10**, doi:10.3390/biom10030421 (2020).

22 Soto, C. *et al.* High frequency of shared clonotypes in human B cell receptor repertoires. *Nature* **566**, 398-402, doi:10.1038/s41586-019-0934-8 (2019).

23 Ou, J. *et al.* Emergence of RBD mutations in circulating SARS-CoV-2 strains enhancing the structural stability and human ACE2 receptor affinity of the spike protein. *bioRxiv*, 2020.2003.2015.991844, doi:10.1101/2020.03.15.991844 (2020).

24 Yuan, M. *et al.* Structural basis of a public antibody response to SARS-CoV-2. *bioRxiv*, 2020.2006.2008.141267, doi:10.1101/2020.06.08.141267 (2020).

25 Horns, F. *et al.* Lineage tracing of human B cells reveals the in vivo landscape of human antibody class switching. *Elife* **5**, doi:10.7554/eLife.16578 (2016).

26 Wardemann, H. *et al.* Predominant autoantibody production by early human B cell precursors. *Science* **301**, 1374-1377, doi:10.1126/science.1086907 (2003).

27 Zhang, J., Kobert, K., Flouri, T. & Stamatakis, A. PEAR: a fast and accurate Illumina Paired-End reAd mergeR. *Bioinformatics* **30**, 614-620, doi:10.1093/bioinformatics/btt593 (2014).

28 Sievers, F. & Higgins, D. G. Clustal Omega for making accurate alignments of many protein sequences. *Protein Sci* **27**, 135-145, doi:10.1002/pro.3290 (2018).

29 Sievers, F. *et al.* Fast, scalable generation of high-quality protein multiple sequence alignments using Clustal Omega. *Mol Syst Biol* **7**, 539, doi:10.1038/msb.2011.75 (2011).

30 Lefranc, M. P. IMGT databases, web resources and tools for immunoglobulin and T cell receptor sequence analysis, http://imgt.cines.fr. *Leukemia* **17**, 260-266, doi:10.1038/sj.leu.2402637 (2003).

31 Ye, J., Ma, N., Madden, T. L. & Ostell, J. M. IgBLAST: an immunoglobulin variable domain sequence analysis tool. *Nucleic Acids Res* **41**, W34-40, doi:10.1093/nar/gkt382 (2013).

32 Kim, S. *et al.* Efficient Selection of Antibodies Reactive to Homologous Epitopes on Human and Mouse Hepatocyte Growth Factors by Next-Generation Sequencing-Based Analysis of the B Cell Repertoire. *Int J Mol Sci* **20**, doi:10.3390/ijms20020417 (2019).

33 Gupta, N. T. *et al.* Hierarchical Clustering Can Identify B Cell Clones with High Confidence in Ig Repertoire Sequencing Data. *J Immunol* **198**, 2489-2499, doi:10.4049/jimmunol.1601850 (2017).

34 Andris-Widhopf, J., Steinberger, P., Fuller, R., Rader, C. & Barbas, C. F., 3rd. Generation of human scFv antibody libraries: PCR amplification and assembly of light- and heavy-chain coding sequences. *Cold Spring Harb Protoc* **2011**, doi:10.1101/pdb.prot065573 (2011).

35 Lee, Y., Kim, H. & Chung, J. An antibody reactive to the Gly63-Lys68 epitope of NT-proBNP exhibits O-glycosylation-independent binding. *Exp Mol Med* **46**, e114, doi:10.1038/emm.2014.57 (2014).

36 Carlos F. Barbas III , D. R. B., Jamie K. Scott , Gregg J. Silverman. Phage Display: A Laboratory Manual. *Cold Spring Harbor Laboratory Press* **76**, 487-488, doi:https://doi.org/10.1086/420571 (2001).

37 Lee, S. *et al.* An antibody to the sixth Ig-like domain of VCAM-1 inhibits leukocyte transendothelial migration without affecting adhesion. *J Immunol* **189**, 4592-4601, doi:10.4049/jimmunol.1103803 (2012).

38 Park, S., Lee, D. H., Park, J. G., Lee, Y. T. & Chung, J. A sensitive enzyme immunoassay for measuring cotinine in passive smokers. *Clin Chim Acta* **411**, 1238-1242, doi:10.1016/j.cca.2010.04.027 (2010).

39 Park, W. B. *et al.* Virus Isolation from the First Patient with SARS-CoV-2 in Korea. *J Korean Med Sci* **35**, e84, doi:10.3346/jkms.2020.35.e84 (2020).

40 REED, L. J. & MUENCH, H. A SIMPLE METHOD OF ESTIMATING FIFTY PER CENT ENDPOINTS12. *American Journal of Epidemiology* **27**, 493-497, doi:10.1093/oxfordjournals.aje.a118408 (1938).

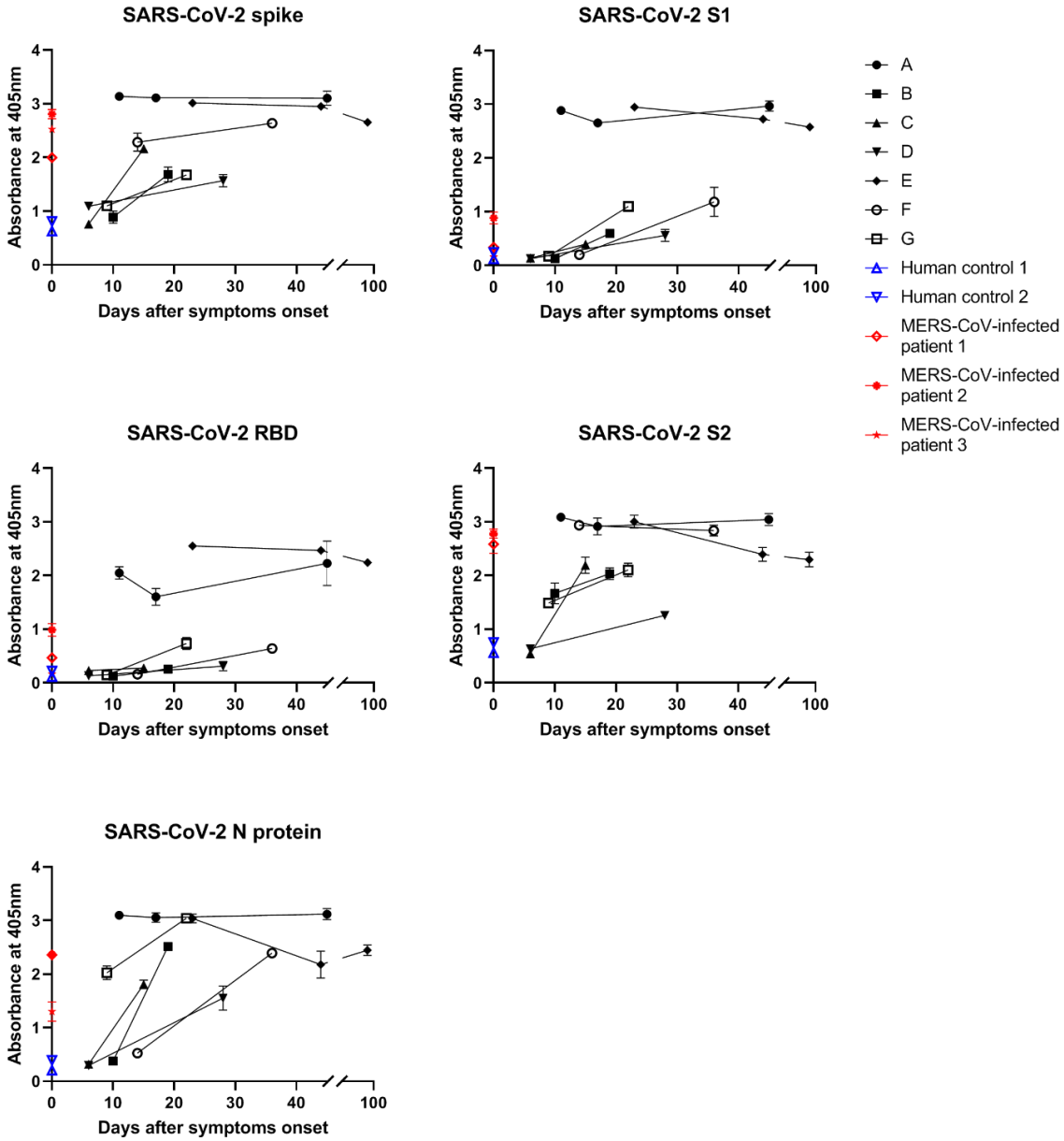

Supplementary Fig 1. Titrations of serum IgG in ELISA.

Plasma samples from seven SARS-CoV-2 patients were diluted (1:100) and added to plates coated with recombinant SARS-CoV-2 spike, S1, S2, or N proteins, fused to HIS tag, or RBD protein, fused to human Cκ domain. The amount of bound IgG was determined using anti-human IgG (Fc-specific) antibody. ABTS was used as the substrate. All experiments were performed in duplicate, and the data are presented as the mean ± SD.

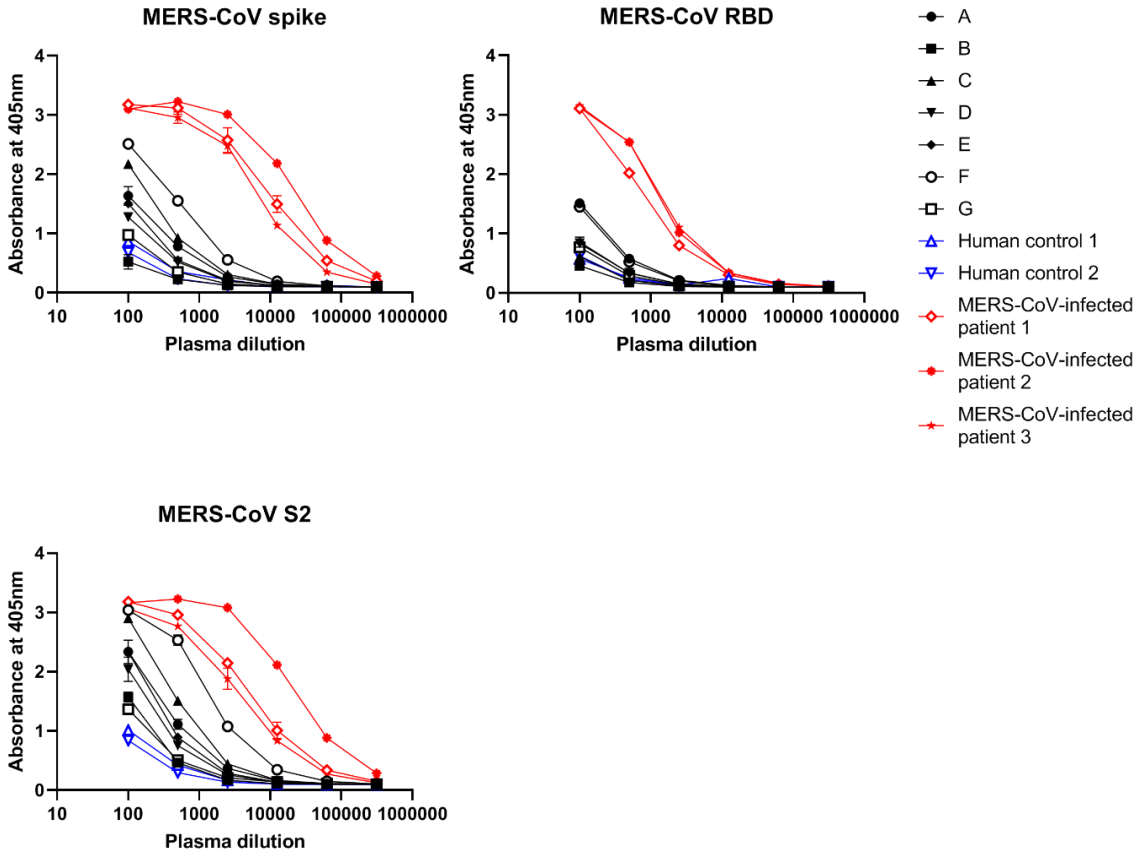

Supplementary Fig 2. Titrations of serum IgG in ELISA.

Plasma samples of seven SARS-CoV-2 patients were serially diluted and added to plates coated with recombinant MERS-CoV spike, RBD, and S2 proteins, fused to HIS. The amount of bound IgG was determined using anti-human IgG (Fc-specific) antibody. ABTS was used as the substrate. All experiments were performed in duplicate, and the data are presented as the mean ± SD.

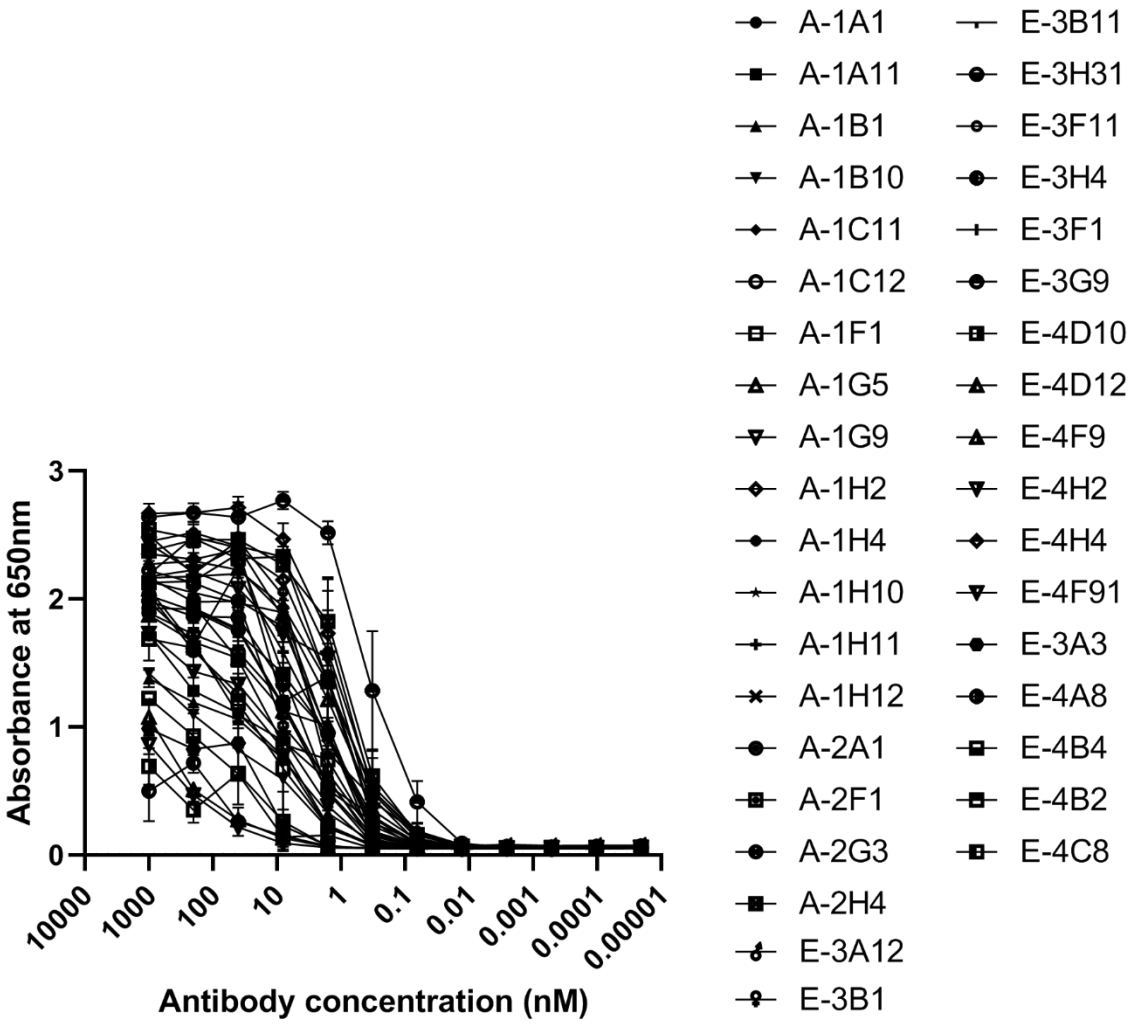

Supplementary Fig 3. Reactivity of anti-SARS-CoV-2 scFv antibodies against recombinant SARS-CoV-2 RBD.

Recombinant SARS-CoV-2 RBD-coated microtiter plates were incubated with varying concentrations of scFv-hCκ fusion proteins. HRP-conjugated anti-human Ig kappa light chain antibody was used as the probe, and TMB was used as the substrate. All experiments were performed in duplicate, and the data are presented as the mean ± SD.

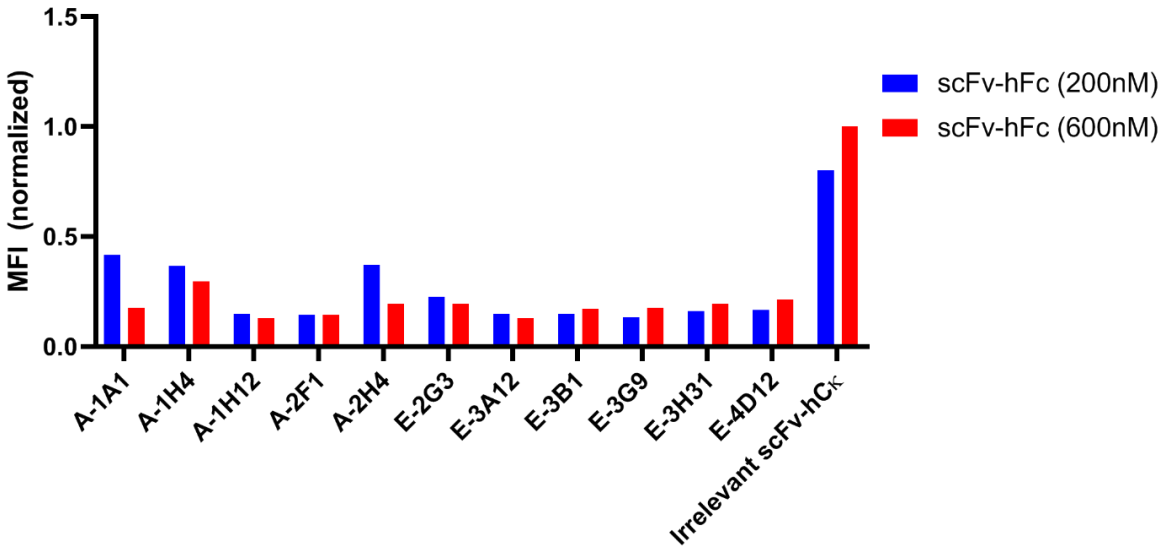

Supplementary Fig 4. Inhibition of recombinant SARS-CoV-2 S glycoprotein binding to ACE2-expressing cells, by flow cytometry.

The recombinant scFv-hFc fusion proteins (200 nM or 600 nM) were mixed and incubated with recombinant SARS-CoV-2 S glycoprotein (200 nM) fused with a HIS tag at the C-terminus. After incubation with Vero E6 ($ACE2^{+}$) cells, the relative amount of bound, recombinant SARS-CoV-2 S glycoprotein was measured using a FITC-conjugated anti-HIS antibody. For each sample, 10,000 cells were monitored.

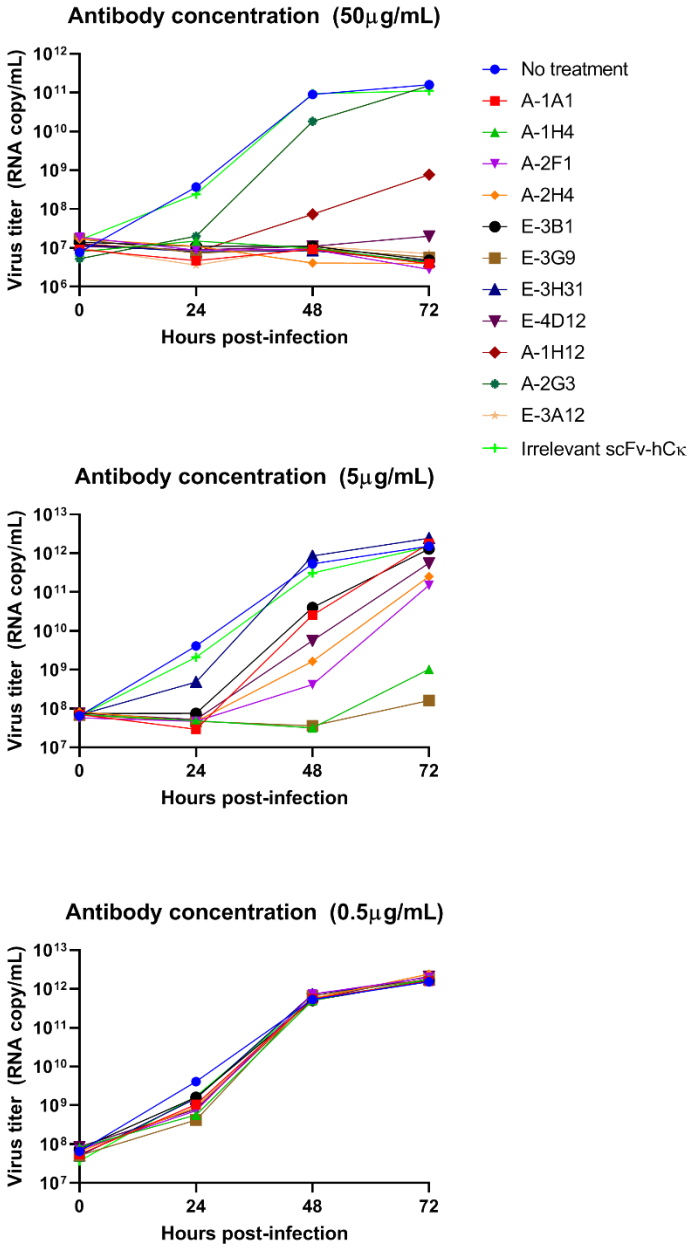

Supplementary Fig 5. Neutralization of SARS-COV-2 in an *in vitro* experiment.

The recombinant scFv-hCκ fusion proteins were mixed with 2,500 $TCID_{50}$ of SARS-CoV-2 (BetaCoV/Korea/SNU01/2020, accession number MT039890), and the mixture was added to the Vero cells. After 0, 24, 48, and 72 h of infection, the culture supernatant was collected to measure the viral titers.

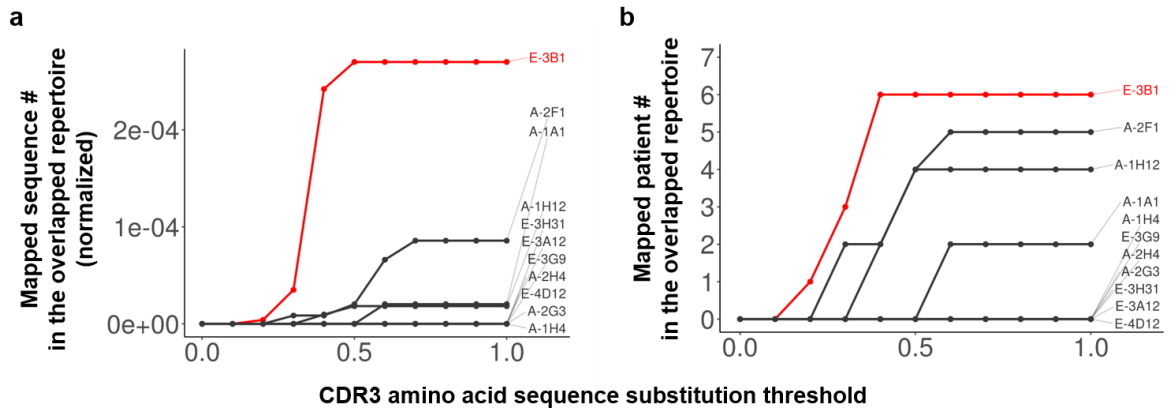

Supplementary Fig 6. Mapping of the 11 nAbs to the overlapping IGH repertoire.

a, The number class-switched IGH sequences in the overlapping repertoire, mapped to nAbs. The allowed number of CDR3 amino acid sequence substitutions during the mapping process is represented on the x-axis of the plot, after normalizing against the sequence length. The number of mapped sequences was normalized against the total number of IGH sequences in each patient, and their sum is represented in the y-axis of the plot. **b,** The number of patients expressing the overlapping class-switched IGH sequences, which were mapped to the nAbs. The x-axis is the same as described for **a** and the y-axis indicates the number of patients.

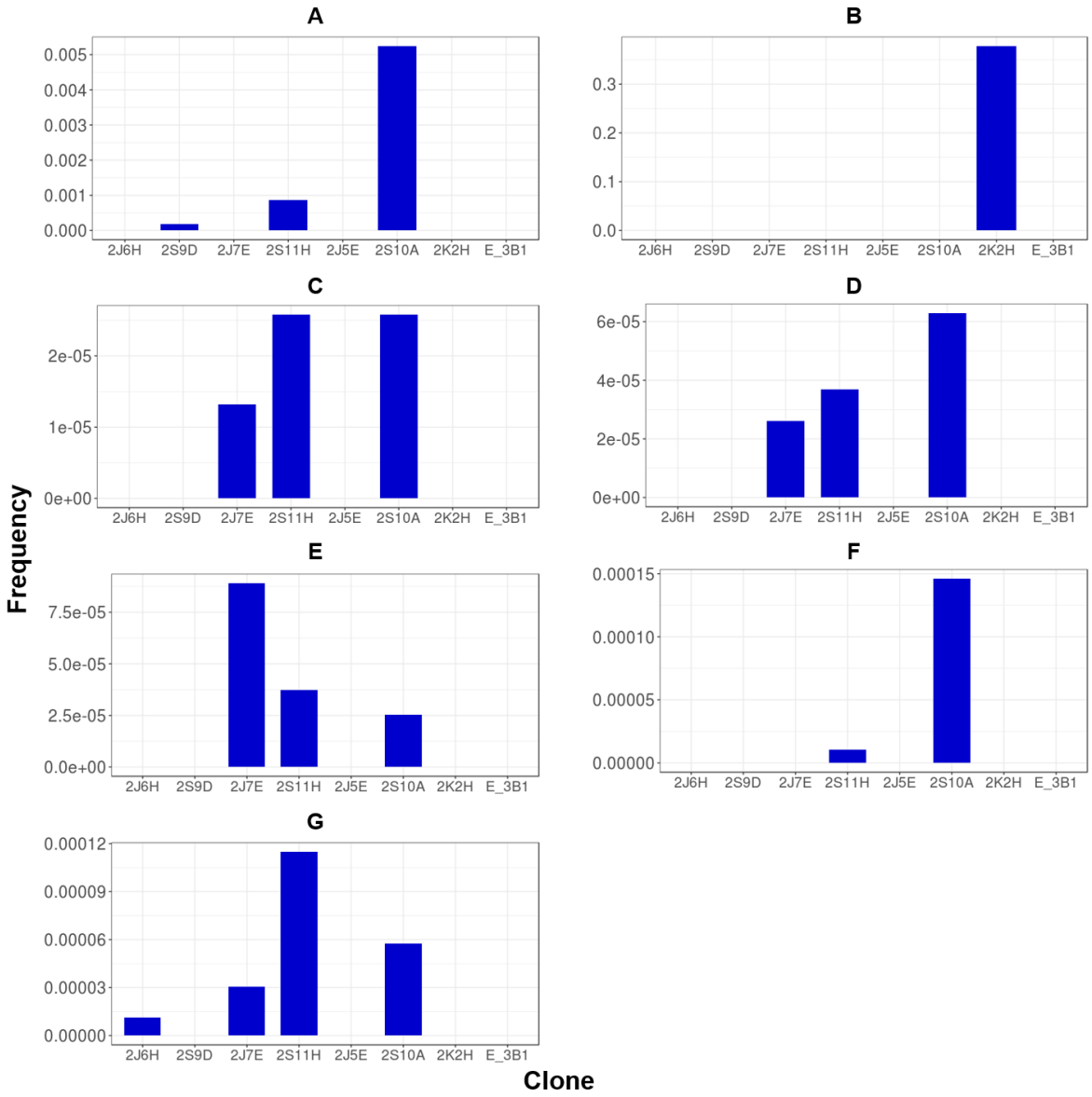

Supplementary Fig 7. Existence of V_L that can be paired with the stereotypic V_H.

V_L was mapped according to identical VJ gene usage and perfectly matched LCDR3 sequences at the amino acid level, which were identified in the IGL repertoires of all seven patients (A–G). The frequency values of the mapped sequences in the repertoires of all sampling points were summed. Patient identification can be found above each bar graph.

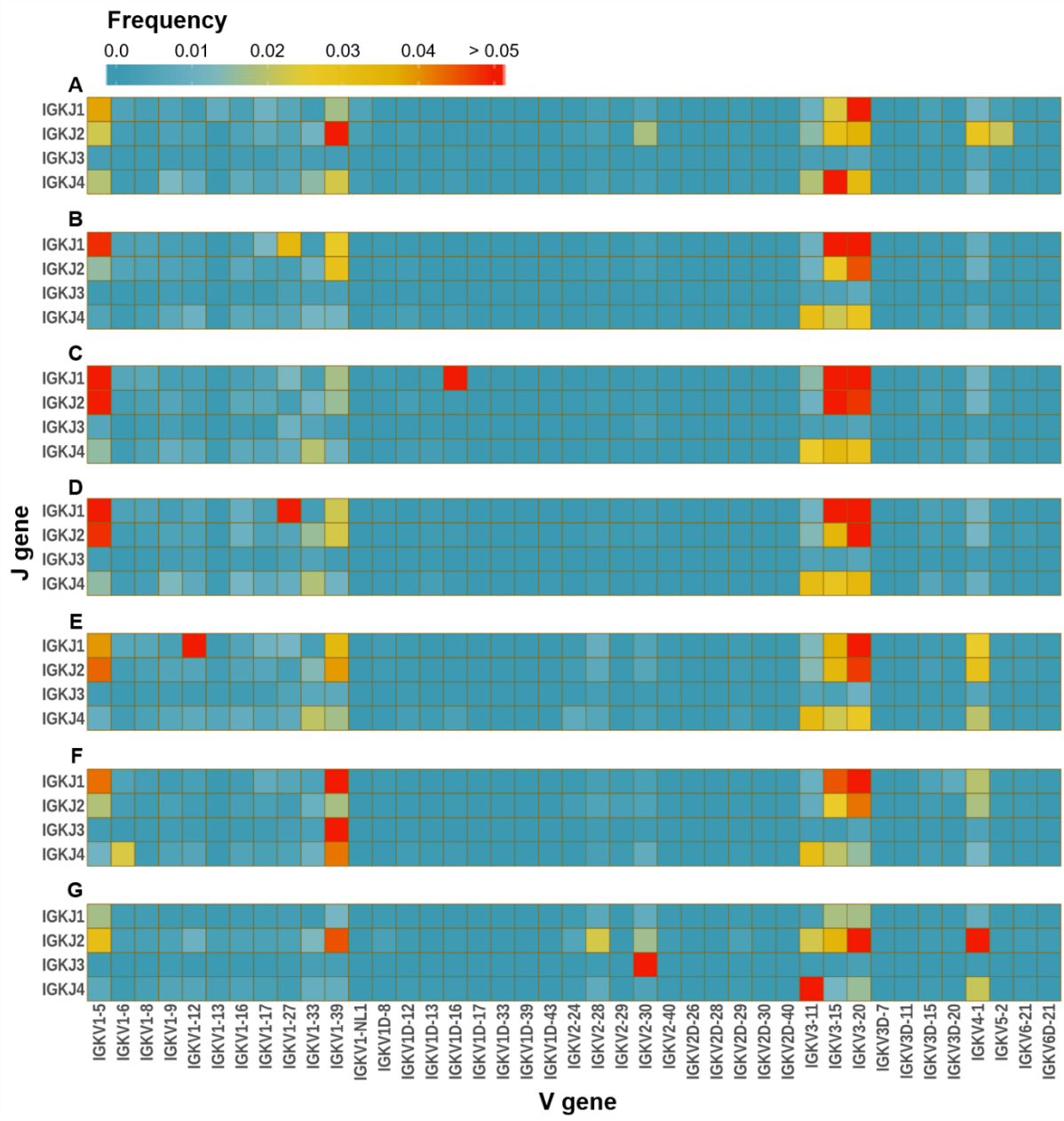

Supplementary Fig 8. VJ gene usage among the IG kappa light chain repertoire of patients.

The frequency values of all sampling points were averaged and represented for each patient. Patient identification can be found at the top left corner of each heatmap.

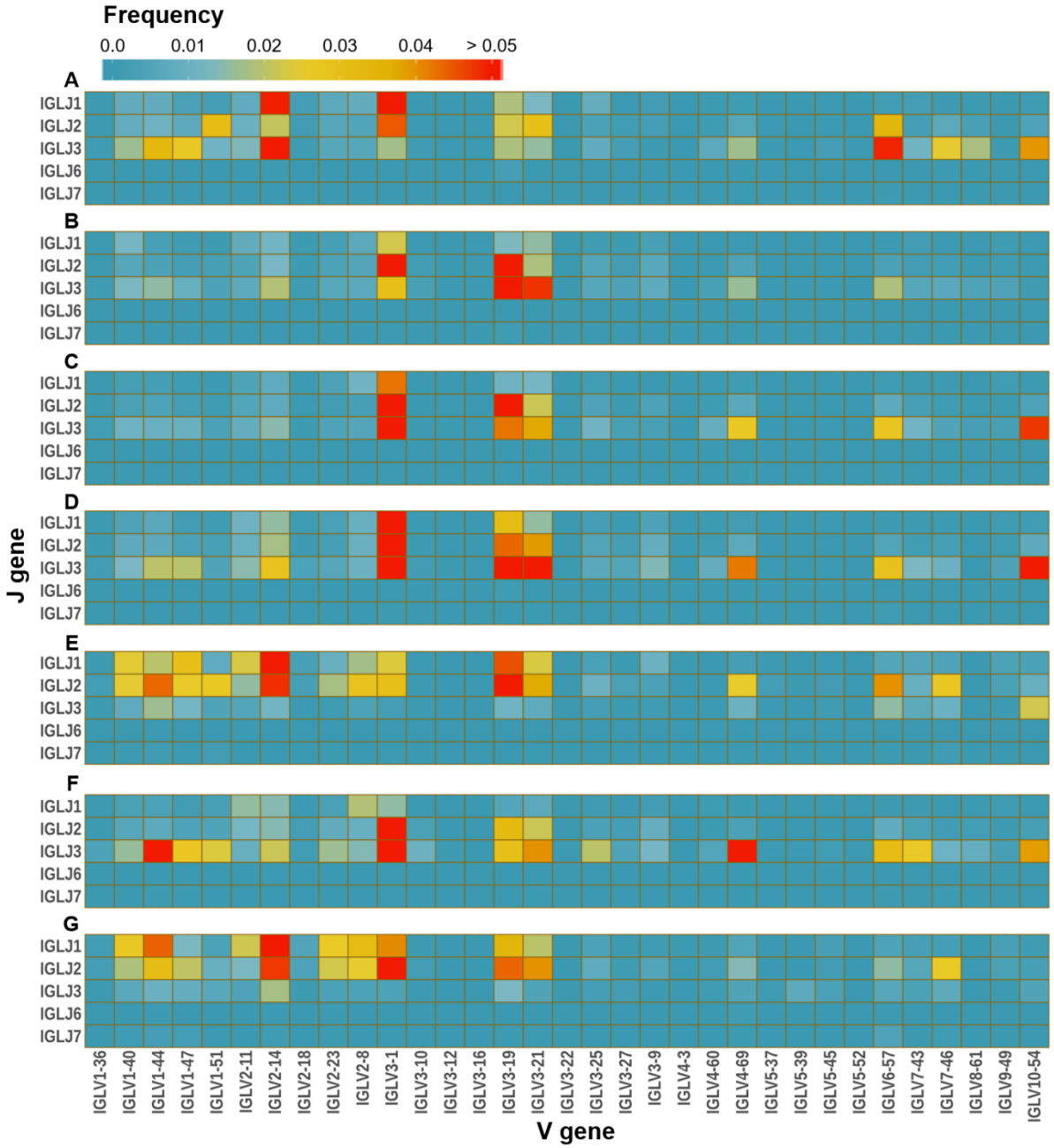

Supplementary Fig 9. VJ gene usage among the IG lambda light chain repertoire of patients.

The frequency values of all sampling points were averaged and are represented for each patient. Patient identification can be found at the left top corner of each heatmap.

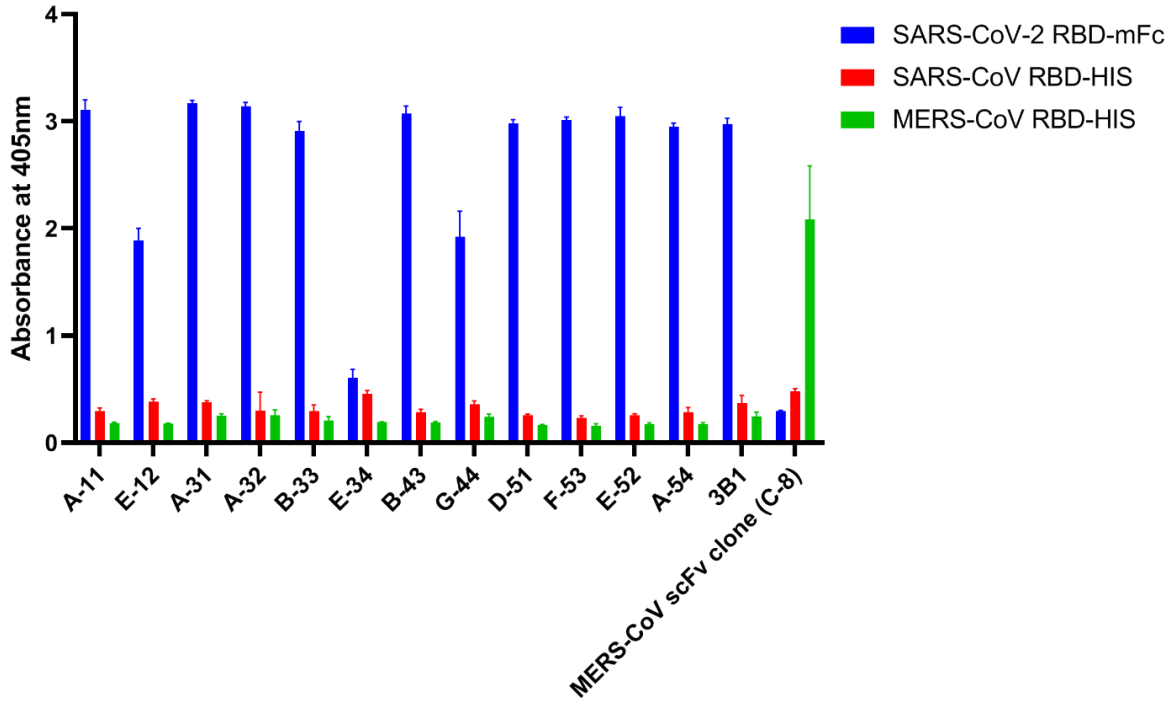

Supplementary Fig 10. Reactivity of phage-displayed scFv clones in phage ELISA.

Recombinant SARS-CoV-2, SARS-CoV, or MERS-CoV RBD protein-coated microtiter plates were incubated with phage clones. HRP-conjugated anti-M13 antibody was used as the probe, and ABTS was used as the substrate. All experiments were performed in quadruplicate, and the data are presented as the mean ± SD.

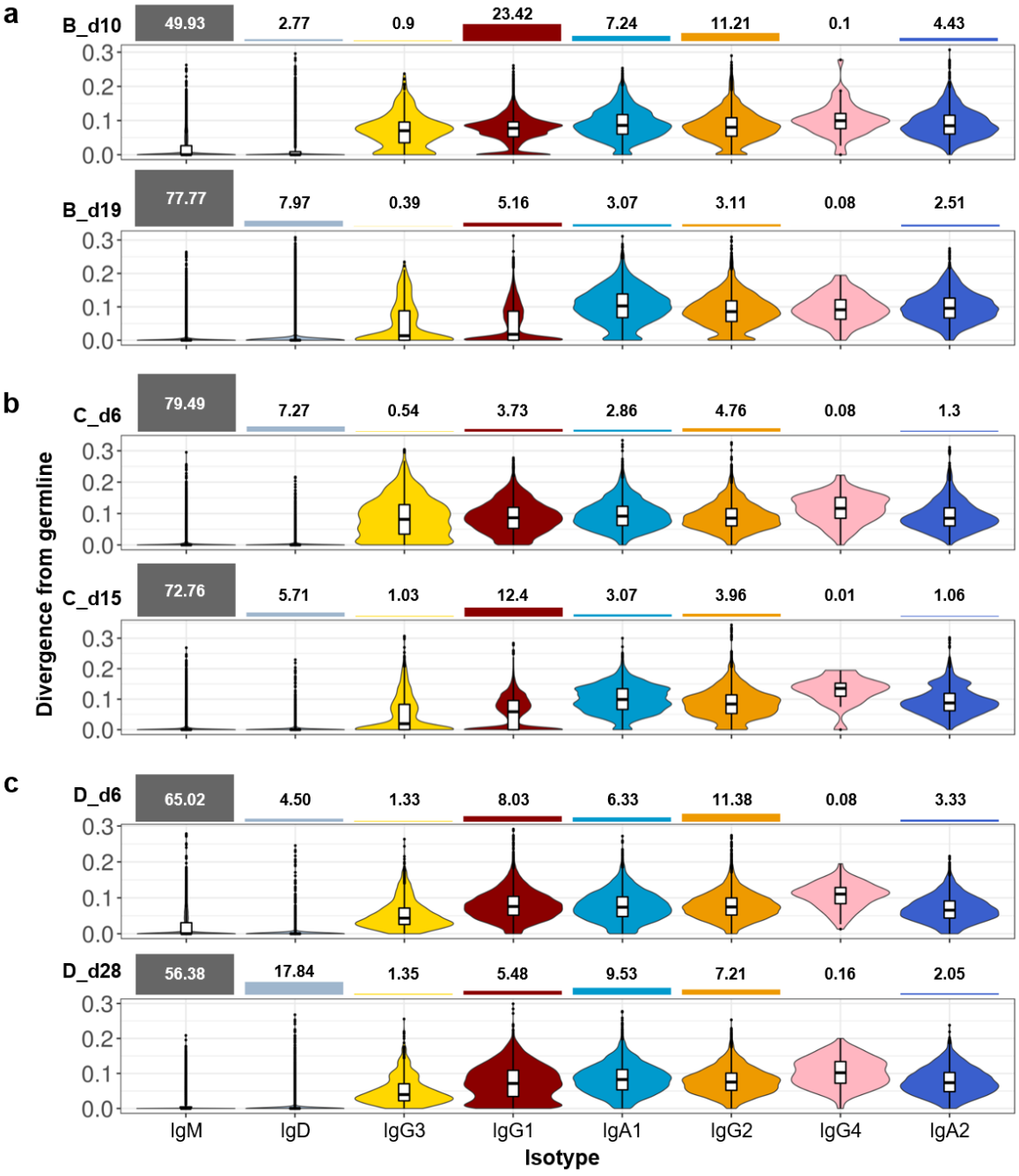

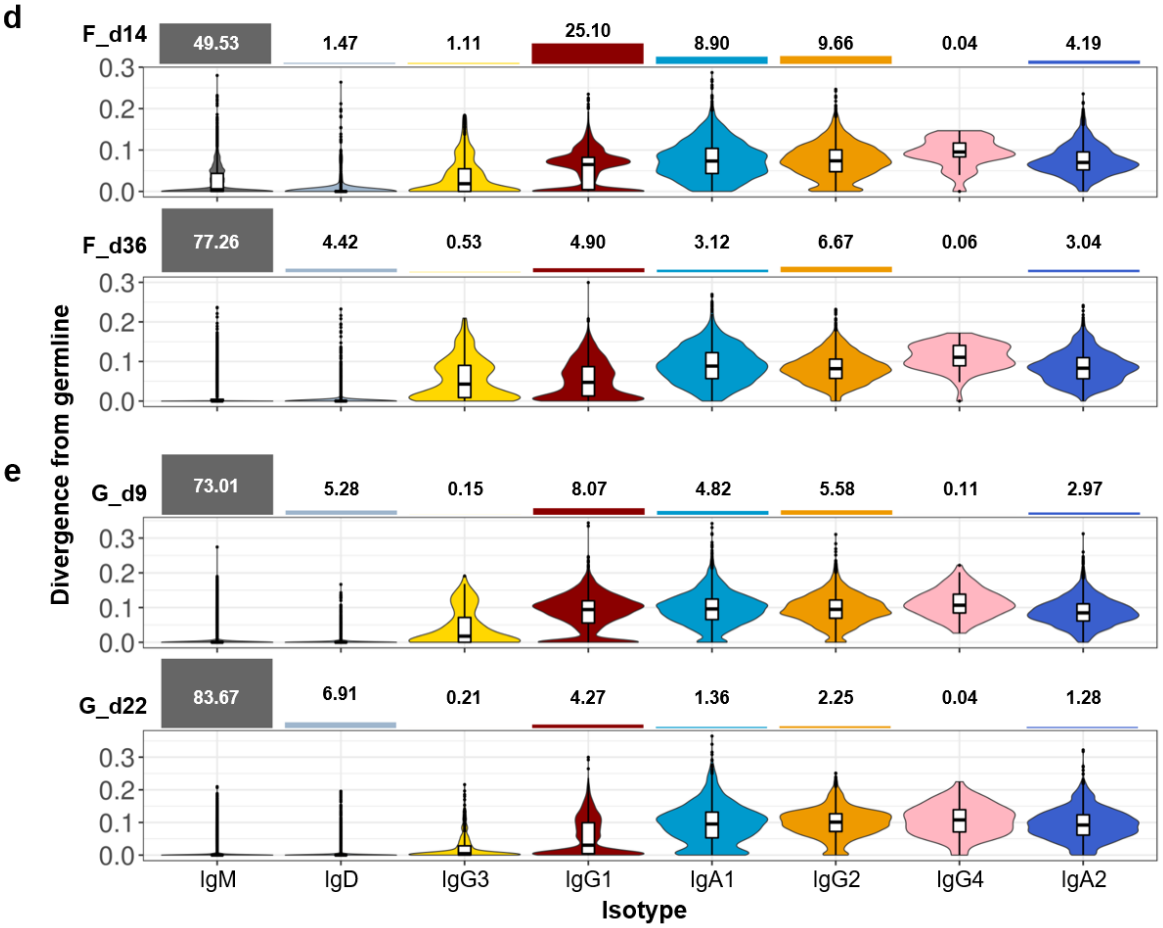

Supplementary Fig 11. Deep profiling of the IGH repertoire of Patients B, C, D, F, and G.

(a-e), IGH repertoires of **a.** Patient B, **b.** Patient C, **c.** Patient D, **d.** Patient F, and **e.** Patient G were examined according to divergence from the germline and the isotype composition of the sequences. Values of divergence from the germline were calculated separately, for each isotype, and are presented as violin plots, class-switching event order. The bar graphs above the violin plots represent the proportions of each isotype.

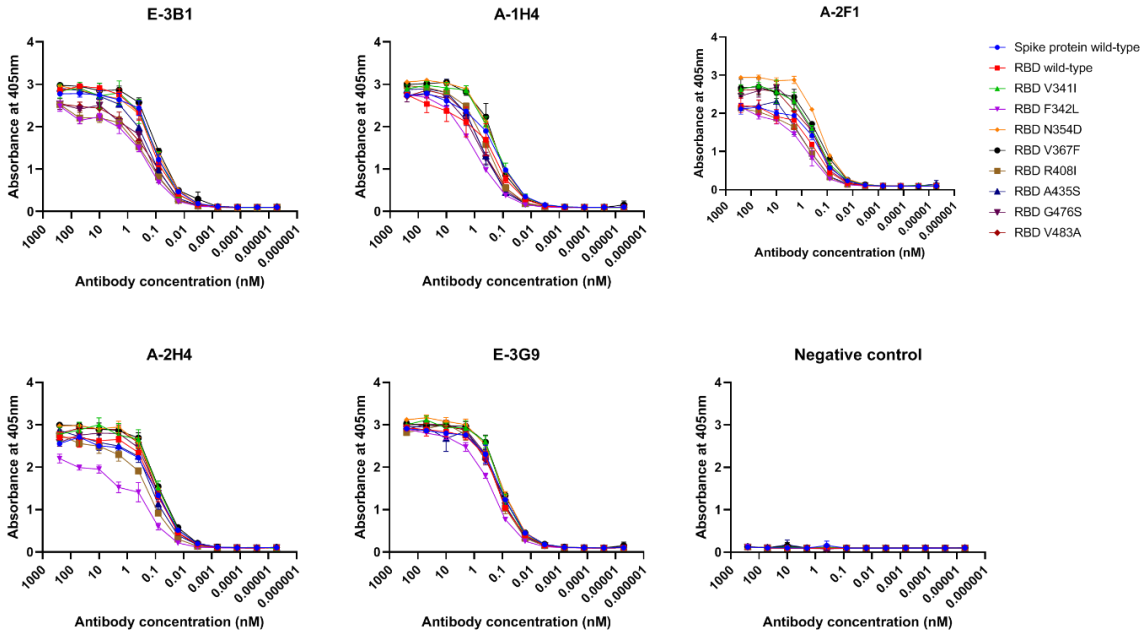

Supplementary Fig 12. Reactivity of nAbs against recombinant SARS-CoV-2 RBD mutants.

Recombinant wild-type or mutant (V341I, F342L, N354D, V367F, R408I, A435S, G476S, and V483A) SARS-CoV-2 RBD protein-coated microtiter plates were incubated with varying concentrations of scFv-hFc fusion proteins. HRP-conjugated anti-human IgG antibody was used as the probe, and ABTS was used as the substrate. All experiments were performed in triplicate, and the data are presented as the mean ± SD.

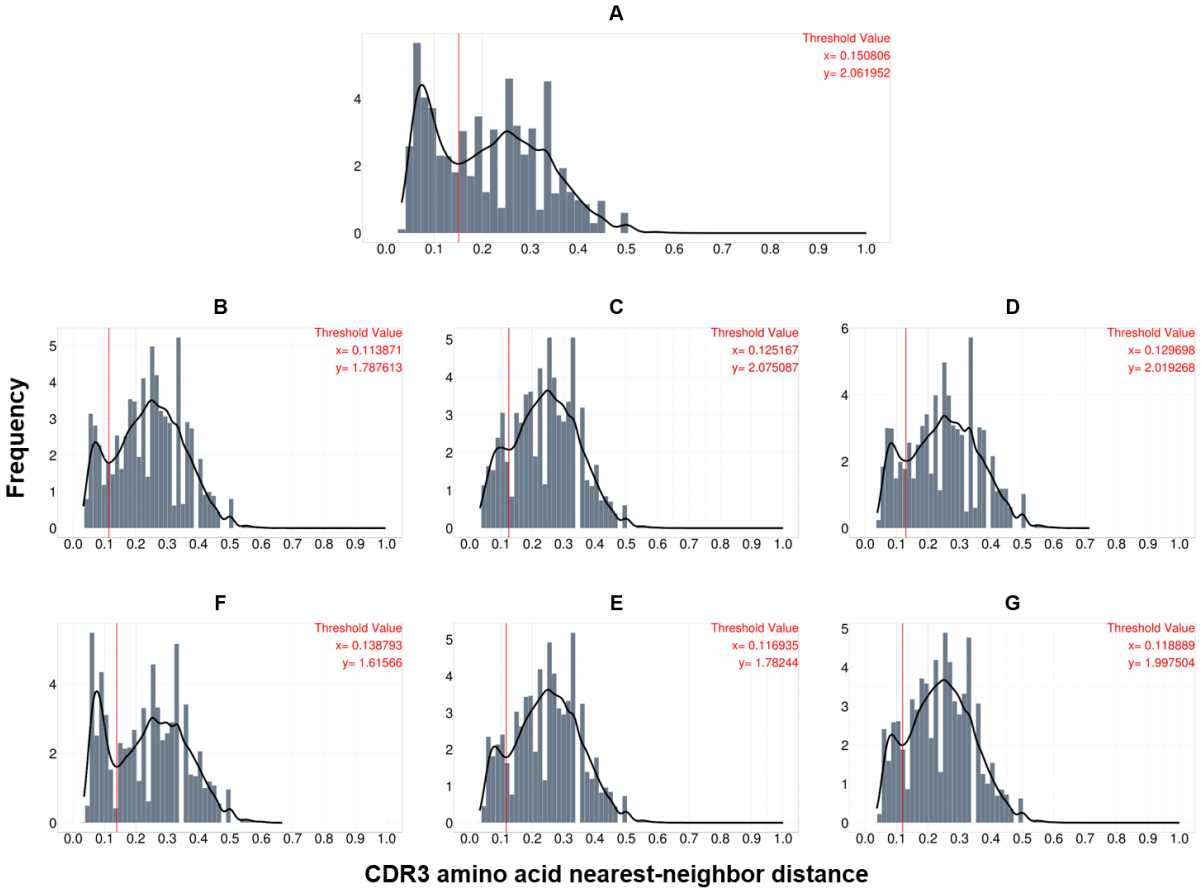

Supplementary Fig 13. The nearest-neighbor distance histogram for HCDR3 amino acid sequences in the IGH repertoires of patients.

The frequency values of the histograms were approximated by the binned kernel estimation method, in the Gaussian kernel setting (black line). The threshold value for each patient was set as the x value of the points with a minimum frequency value between two peaks of the bimodal distribution (red vertical line). The x and y values of the threshold-setting point are indicated in the upper right corner of each histogram.

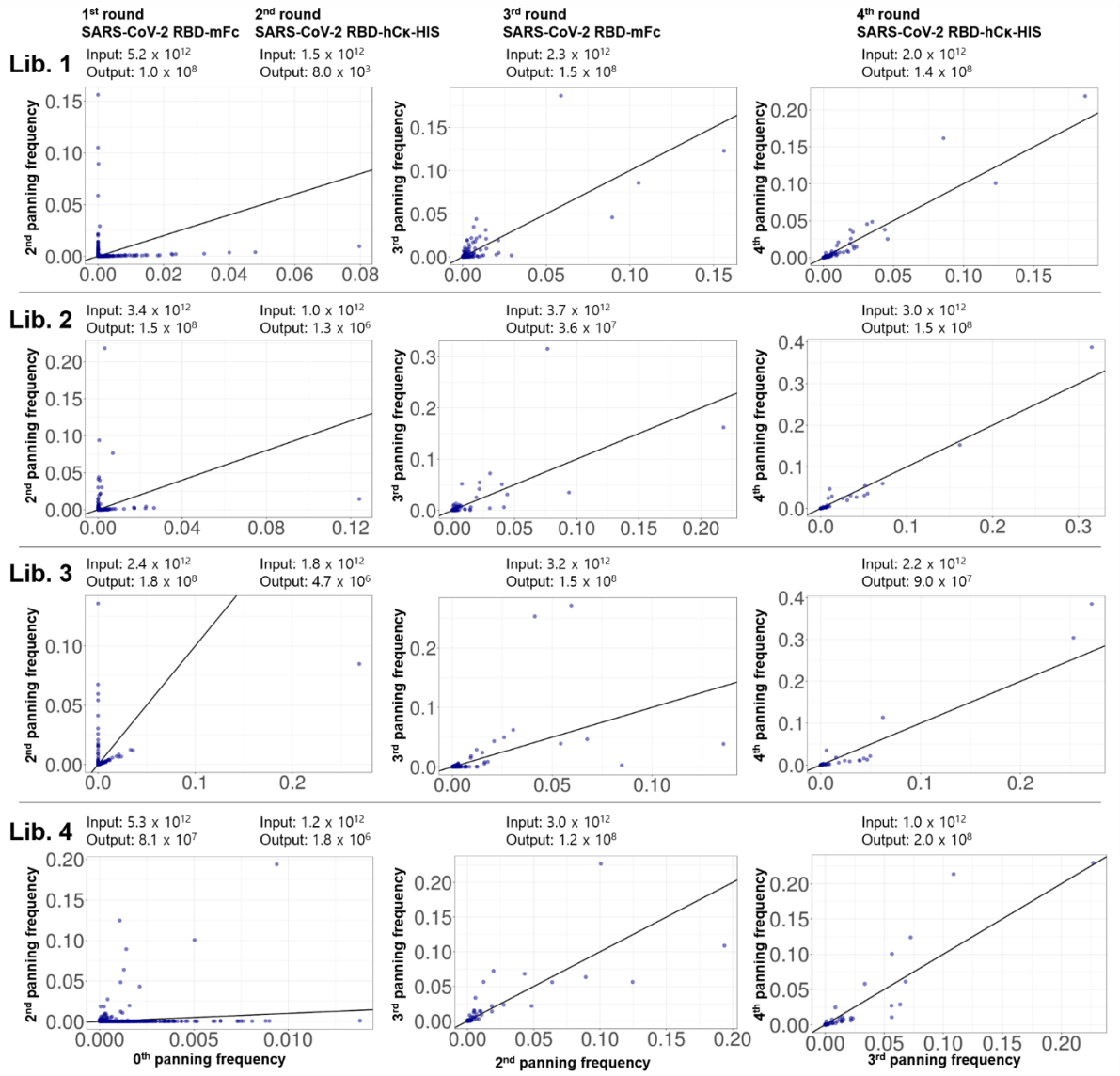

Supplementary Fig 14. Frequency scatter plots for the NGS data of the four libraries, after each round of biopanning.

The x- and y-axes represent the frequency values for the NGS data in each biopanning round. The line on the scatter plots indicates the identity line (y = x). Input and output virus titer values are also presented, above the matched scatter plots.

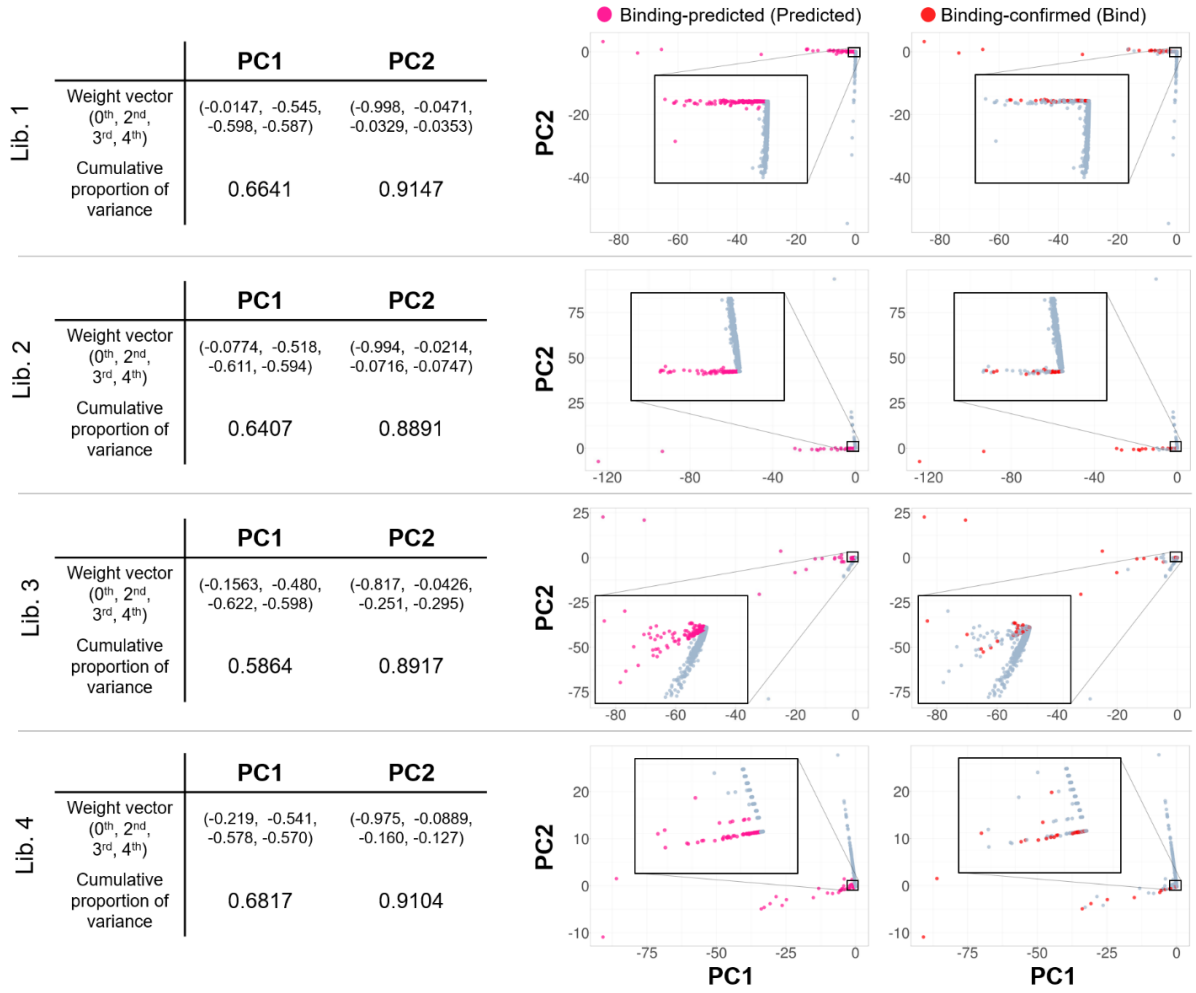

Supplementary Fig 15. The results of principal component analysis, applied to the NGS data of four libraries, after each round of biopanning.

Information regarding the PC weight vectors and the cumulative proportion of variance explained by the PCs are listed on the left side of the plots. PCA plots for PC1 and PC2 on shown on the right side of the plots. The binding-predicted clones were defined based on the value of PC1 and the ratio between PC1 and PC2, by setting a constant threshold value for each. The population of clones defined as predicted clones is marked in pink. The clones known bind to SARS-CoV-2 RBD are marked in red.

Supplementary Table 1. Demographic and clinical characteristics

Patient no.	A	B	C	D	E	F	G
Age	55	55	53	24	48	40	59
Sex	Male	Male	Female	Male	Male	Female	Female
Race	Korean	Korean	Korean	Korean	Chinese	Chinese	Korean
BMI (kg/m^2)	31.35	24.09	23.10	21.51	27.02	22.15	18.00
Underlying diseases	-	DM, HTN, DL	-	-	-	-	DM, DL
Highest temperature (°C)	39.7	38.4	38.0	37.8	37.8	37.8	37.0
Symptoms	Dyspnea, myalgia, diarrhea	Sputum, myalgia	Sputum, myalgia	Myalgia	Cough, myalgia, diarrhea	Cough, sputum, myalgia, diarrhea	-
Pneumonic infiltrates	Extensive	Limited	Limited	Limited	Extensive	Limited	Limited
Oxygen therapy	Yes	No	No	No	No	No	No
Ventilator	No	No	No	No	No	No	No
Antiviral Treatment	Lopinavir/ ritonavir	-	-	-	Lopinavir/ ritonavir	Lopinavir/ ritonavir	-
Antibiotic Treatment	Levofloxacin	-	-	-	-	-	-
Blood samples collected after symptoms onset (Days)	11, 17, 45	10, 19	6, 15	6, 28	23, 44, 99	14, 36	9, 22

BMI, body mass index; DM, diabetes mellitus; HTN, hypertension; DL, dyslipidemia

Supplementary Table 2. SARS-CoV-2 RBD-reactive scFv clones

Clone	HCDR1	HCDR2	HCDR3	V gene	J gene	Divergence	Mapped patient	Mapped isotype
E_3B1	SNYMS	VLYSGGSTFYADSVKG	DAQVYGMDV	IGHV3-66	IGHJ6	0.023973	E	G1
E_3A3	RNYMS	VIYSGGSTYYADSVKG	DLDTAGGMDV	IGHV3-66	IGHJ6	0.010239	-	-
E_3H4	SNYMS	VIYSGGSTYYADSVKG	DLLEQGGMDV	IGHV3-66	IGHJ6	0.006826	E	G1
A_2F1	SNYMS	VIYSGGSTFYADSVKG	DLMEAGGMDV	IGHV3-53	IGHJ6	0.030822	-	-
A_1H4	SNYMS	GIYSGGSTYYADSVKG	DLQEAGAFDI	IGHV3-66	IGHJ3	0.027304	-	-
E_4H2	SYWMS	NIKQDGSEKYYVDSVKG	HRWLRGEIDY	IGHV3-7	IGHJ4	0.003401	E	G1
A_1G5	DYYMS	VISYDGSNKYYADSVKG	SSWLRGAFDY	IGHV3-30	IGHJ4	0.061017	-	-
E_4G3	SYWIG	IIYPGDSDTRYSPSFQG	LSSSYYGWFDP	IGHV5-51	IGHJ5	0.006826	-	-
E_3B11	SYWIA	IIYPGDSDTRYSPSFQG	YSSSPNGWFDP	IGHV5-51	IGHJ5	0.010239	E	G1
A_1C12	SNAIS	RIIPIFGTANYAQKFQG	DVIESPLYGMDV	IGHV1-69	IGHJ6	0.027027	A	G1
E_4B2	SFAIT	RIIPILGIANYAQKFQG	EFSGGDNTGFDY	IGHV1-69	IGHJ4	0.023649	E	G1
E_4D10	SHYMH	IINPSGGSTSYAQKFQG	DGYFVPARSAFDI	IGHV1-46	IGHJ3	0.013652	E	M
A_2A1	DYAMH	GISWNSGTIGYADSVKG	DITMVREAYGMDV	IGHV3-9	IGHJ6	0.033557	-	-
A_1H11	DYAMH	GTSWNSGTIGYADSVKG	DKGQIRESYGMDV	IGHV3-9	IGHJ6	0.071186	-	-
A_1B10	DYAMH	GTDWNSGTIGYADSVKG	DLGGVVERYGMDV	IGHV3-9	IGHJ6	0.031802	-	-
A_1H10	SYYIH	IINPDAGSTTYAQKFQG	DLYGLPGRAAFDI	IGHV1-46	IGHJ3	0.037288	-	-
E_3A12	SNYMS	VIYSGGSTYYADSVKG	GDGSGDYYYGMDV	IGHV3-53	IGHJ6	0.006849	E	A2
A_1B1	NYWIG	IIYPGDSDTRYSPSFQG	HLDWNAPRGPFDI	IGHV5-51	IGHJ3	0.013699	-	-
A_1C11	DYAMH	GISWNSGTIGYADSVKG	DIFRTEWLQYGMDV	IGHV3-9	IGHJ6	0.027119	-	-
E_3F11	DYAMH	GSSWNSGTIGYADSVKG	DMGRGNDNNLAFDI	IGHV3-9	IGHJ3	0.037543	E	G1
E_3G9	SYYMH	IINPSGGSTSYAQKFQG	EGVWDSSGYSSFDY	IGHV1-46	IGHJ4	0.013514	E	A1
E_4C8	DYAMH	GVTWNSGSIGYADSVKG	DISPMLRGDNYGMDV	IGHV3-9	IGHJ6	0.016949	E	G1
E_4A8	DYAMH	SVTWNSGNIGYADSVKG	DISSMLRGDNYCMDV	IGHV3-9	IGHJ6	0.047619	-	-
E_3F1	SYAIS	RIIPILGIANYAQKFQG	DRGYSDYGSNPFFDY	IGHV1-69	IGHJ4	0.047458	-	-
E_4H4	SYAIS	RIIPILGIANYAQKFQGX	GIGYSGSGSNDYFDS	IGHV1-69	IGHJ4	0.03367	-	-
A_1F1	DYAMH	GISWNSGIIGYADSVKG	DIRGYSGYDDPGAFDI	IGHV3-9	IGHJ3	0.010067	-	-
E_4B4	DYAMH	GSSWNSGSIGYADSVKG	GKSPLDYDQTMGAFDI	IGHV3-9	IGHJ3	0.027119	E	A1
A_1A11	DYAMS	FIRSKAYGGTTEYAASVKG	DEDSGTLLPGFYYYDMDV	IGHV3-49	IGHJ6	0.003322	A	G1
E_4D12	TYWIN	RIDPSDSYTNYSPSFQG	GDYYDNSDYSGLSEYFQH	IGHV5-10-1	IGHJ1	0.013605	E	G1
E_3H31	RYAMH	WINAGNGKTKYSQKFQG	ALYYYDSSGSTQSDDAFDI	IGHV1-3	IGHJ3	0.016949	E	G1
E_4F91	SNYMS	VIYSGGSTYYADSVKG	DGQRMAAAGTEDYYYGMDV	IGHV3-66	IGHJ6	0.003413	E	G1|A1|A2
A_1H12	DYAMH	GVTWNSGTIGYADSVKG	DIMGDGSPSLHYYYYGMDV	IGHV3-9	IGHJ6	0.033557	-	-
E_4F9	SNYMS	VIYIGGSTYYSYSVKG	DRQRMAAAGTEDYYYGMDV	IGHV3-66	IGHJ6	0.044369	-	-
A_2G3	DYGMT	GINWNGGTTGYADSVKG	IYCGDDCYSLVIWGDAFDI	IGHV3-20	IGHJ3	0.023891	-	-
A_1A1	DYAMH	GISWNSGTIGYADSVKG	DENRGYSSRWYDPEYYGMDV	IGHV3-9	IGHJ6	0.006826	A	G1
A_2H4	VYGMH	VISYDGSNKYYADSVKG	GGPRPVVKAYGELDYYGMDV	IGHV3-30	IGHJ6	0.030928	-	-
A_1G9	DYAMH	GTSWNSGTIGYADSVRG	YGTEGLYDFRSGYGHYGMDV	IGHV3-9	IGHJ6	0.03413	-	-
A_1H2	RYAIS	GIIPIFGTANYAQKFQG	ERTYCSSTSCYAGYYYYGMDV	IGHV1-69	IGHJ6	0.016892	A	G1|A1

Supplementary Table 3. Class-switched IGH clonotypes homologous to E-3B1

Patient	HCDR1	HCDR2	HCDR3	V gene	J gene	Divergence	Isotype	Substitution in HCDR3
A	SNYMS	VIYSGGSTYYADSVKG	DLAVYGMDV	IGHV3-53	IGHJ6	0.004386	G1	0.222222
A	SNYMS	VIYSGGSTYYADSVKG	DLDYYGMDV	IGHV3-53	IGHJ6	0	G1	0.333333
A	SNYMS	VIYSGGSTFYADSVKG	DLGDYGMDV	IGHV3-53	IGHJ6	0.008772	G1	0.333333
A	SNYMS	VIYSGGSTYYADSVKG	DLQVYGMDV	IGHV3-53	IGHJ6	0	G1	0.111111
A	SNYMS	DIYSGGSTDYADSVKG	DLSYYGMDV	IGHV3-53	IGHJ6	0.008772	G1	0.333333
A	SNYMS	VIYSGGSTYYADSVKG	DLSYYGMDV	IGHV3-53	IGHJ6	0	G1	0.333333
A	SNYMN	VIYSGGSTFYADSVKG	DLSYYGMDV	IGHV3-53	IGHJ6	0.030702	G1	0.333333
A	SNYMS	VIYSGGSTYYADSVKG	DLVAYGMDV	IGHV3-53	IGHJ6	0	G1	0.333333
A	SNYMS	VIYAGGTTDYADSVKG	DLVAYGMDV	IGHV3-53	IGHJ6	0.039474	G1	0.333333
A	SNYMS	VIYSGGSTYYADSVKG	DLVDYGMDV	IGHV3-53	IGHJ6	0	G1	0.333333
A	SNYMS	VIYSGGSTYYADSVKG	DLVIYGMDV	IGHV3-53	IGHJ6	0	G1	0.333333
A	SNYMS	VIYSGGSTYYADSVKG	DLVIYGMDV	IGHV3-53	IGHJ6	0.008772	G1	0.333333
A	SNYMS	VIYSGGSTYYADSVKG	DLVIYGMDV	IGHV3-53	IGHJ6	0	G1	0.333333
A	SNYMS	VIYSGGSTYYADSVKG	DLVIYGMDV	IGHV3-53	IGHJ6	0.004386	G1	0.333333
A	SNYMS	VIYSGGSTYYADSVKG	DLVVMGMDV	IGHV3-53	IGHJ6	0	G1	0.333333
A	SNYMS	VIYSGGSTYYADSVKG	DLYYYGMDV	IGHV3-53	IGHJ6	0	G1	0.333333
A	SNYMS	VIYSGGSTYYADSVKG	DLYYYGMDV	IGHV3-53	IGHJ6	0	G1	0.333333
A	SNYMS	VIYSGGSTYYADSVKG	DLYYYGMDV	IGHV3-53	IGHJ6	0.004386	G1	0.333333
A	SNYMT	IIYSGGSTYYADSVKG	DLYYYGMDV	IGHV3-53	IGHJ6	0.017544	G1	0.333333
A	SNYMS	VIYSGGSTYYADSVKG	DLYYYGMDV	IGHV3-53	IGHJ6	0	G1	0.333333
A	SNYMS	VIYSGGSTFYADSVKG	DLYYYGMDV	IGHV3-53	IGHJ6	0.004386	G1	0.333333
A	SNYMS	IIYSGGSTFYADSVKG	DLYYYGMDV	IGHV3-53	IGHJ6	0.013158	G1	0.333333
A	SNYMS	VIYSGGSTFYADSVKG	DLYYYGMDV	IGHV3-53	IGHJ6	0.004386	G1	0.333333
A	SNYMS	VIYSGGSTYYADSVKG	DRDYYGMDV	IGHV3-53	IGHJ6	0	G1	0.333333
B	SNYMS	VIYSGGSTYYADSVKG	DLVAYGMDV	IGHV3-53	IGHJ6	0.008772	G1	0.333333
B	SNYMS	VIYSGGSTYYADSVKG	DLVVYGMDV	IGHV3-53	IGHJ6	0	G1	0.222222
B	SNYMS	VIYSGGSTDYADSVKG	DLVVYGMDV	IGHV3-53	IGHJ6	0.004386	G1	0.222222
B	SNYMS	VIYSGGSTYYADSVKG	DLVVYGMDV	IGHV3-53	IGHJ6	0	G1	0.222222
B	SNYMS	VIYSGGSTYYADPVKG	DLVVYGMDV	IGHV3-53	IGHJ6	0.004386	G1	0.222222
B	SNYMS	VIYSGGSTYYADSVKG	DLYYYGMDV	IGHV3-53	IGHJ6	0	G1	0.333333
D	SNYMN	VIYSGGSTYYTDSVKG	DLHYYGMDV	IGHV3-53	IGHJ6	0.013158	G1	0.333333
D	SNYMT	VIYSGGSTYYADSVKG	DLVYYGMDV	IGHV3-53	IGHJ6	0.004386	G1	0.333333
E	SNYMS	VIYSGGSTYYADSVKG	DLAVYGMDV	IGHV3-66	IGHJ6	0.017543	G1	0.222222
E	SNYMS	VIYSGGSTYYADSVKG	DLAYYGMDV	IGHV3-66	IGHJ6	0.008772	A1	0.333333
E	SNYMS	VIYSGGTTYYADSVKG	DLDYYGMDV	IGHV3-53	IGHJ6	0.004386	A1	0.333333
E	SNYMS	VIYSGGSIFYADSVKG	DLGDYGMDV	IGHV3-53	IGHJ6	0.030702	A1	0.333333
E	SNYMC	VIYSGGSTYYADSVKG	DLGDYGMDV	IGHV3-53	IGHJ6	0.004386	G1	0.333333
E	SNYMS	VIYSGGSTYYADSVKG	DLGPYGMDV	IGHV3-53	IGHJ6	0.008772	G1	0.333333
E	SNYMS	VIYSGGSTYYADSVKG	DLGSYGMDV	IGHV3-53	IGHJ6	0.008772	A2	0.333333
E	SNYMN	VIYSGGSTYYADSVKG	DLPYYGMDV	IGHV3-66	IGHJ6	0.004386	G1	0.333333
E	SNYMS	VIYSGGSTYYADSVKG	DLTVYGMDV	IGHV3-53	IGHJ6	0.008772	A1	0.222222
E	SNYMS	VIYSGGSTYYADSVKG	DLVAYGMDV	IGHV3-53	IGHJ6	0.004386	G1	0.333333
E	SNYMS	VIYSGGSTYYADSVKG	DLVAYGMDV	IGHV3-53	IGHJ6	0.008772	G1	0.333333
E	SNYMS	VIYSGGSTYYADSVKG	DLVVLGMDV	IGHV3-53	IGHJ6	0.008772	A2	0.333333
E	SNYMT	LIYSGGSTYYADSVKG	DLVVWGMDV	IGHV3-53	IGHJ6	0.039474	G1	0.333333
E	SNYMT	VIYSGGSTYYADSVKG	DLVVYGMDV	IGHV3-53	IGHJ6	0.013158	A2	0.222222
E	SNYMS	VLYSGGSTYYADSVKG	DLVYYGMDV	IGHV3-66	IGHJ6	0.013158	A1	0.333333
F	SNYMS	VIYSGGSTYYADSVKG	DLGDYGMDV	IGHV3-53	IGHJ6	0	G1	0.333333
F	RNYMS	IIYSGGSTFYADSVKG	DLSYYGMDV	IGHV3-53	IGHJ6	0.017544	G1	0.333333
F	SNYMS	VIYSGGSTYYADSVKG	DLVYYGMDV	IGHV3-53	IGHJ6	0	G1	0.333333
F	SNYMS	VIYSGGSTYYADSVKG	DLVYYGMDV	IGHV3-53	IGHJ6	0.004386	G1	0.333333
G	SNYMN	IIYSGGTTYYADSVKG	DLYYYGMDV	IGHV3-66	IGHJ6	0.013274	A1	0.333333
G	SNYMS	VIYSGGSTYYADSVKG	DLYYYGMDV	IGHV3-53	IGHJ6	0.004386	G1	0.333333
G	SNYMS	VIYSGGSTYYADSVKG	DLYYYGMDV	IGHV3-53	IGHJ6	0	A1	0.333333
G	SNYMN	VIYSGGSTYYADSVKG	DVVVWGMDV	IGHV3-53	IGHJ6	0.013158	G1	0.333333

Supplementary Table 4. Human monoclonal antibodies reactive against MERS-CoV RBD

Clone	V gene	J gene	Divergence
4	IGHV3-23	IGHJ4	0.075862
13	IGHV3-23	IGHJ4	0.061224
28	IGHV3-30	IGHJ6	0.013559
34	IGHV3-21	IGHJ3	0.057627
36	IGHV3-23	IGHJ4	0.064626
38	IGHV3-23	IGHJ4	0.088136
42	IGHV3-21	IGHJ4	0.061433
103	IGHV3-23	IGHJ4	0.050847
119	IGHV3-9	IGHJ6	0.087838
180	IGHV6-1	IGHJ4	0.009836
113	IGHV3-30	IGHJ4	0.00339
121	IGHV1-69	IGHJ4	0.128028
6	IGHV4-39	IGHJ5	0.016892
25	IGHV4-39	IGHJ5	0.016892
10-1	IGHV1-69	IGHJ5	0.006757
20-1	IGHV1-69	IGHJ5	0.006757
38-1	IGHV1-69	IGHJ5	0.006757
39	IGHV1-69	IGHJ5	0.010135
40	IGHV1-69	IGHJ5	0.006757
11	IGHV4-39	IGHJ4	0.020067
26	IGHV4-39	IGHJ4	0.036789
21	IGHV1-69	IGHJ5	0.003378
17	IGHV1-69	IGHJ3	0.010135
30	IGHV1-69	IGHJ3	0.020339
33	IGHV1-69	IGHJ3	0.016949
41	IGHV1-69	IGHJ3	0.013514
46	IGHV4-39	IGHJ4	0.016722
47	IGHV4-39	IGHJ4	0.016722
48	IGHV4-39	IGHJ4	0.020067
7	IGHV3-21	IGHJ6	0.010274
9	IGHV1-69	IGHJ4	0.017065
31	IGHV1-69	IGHJ5	0.020339
35	IGHV3-21	IGHJ6	0.006849
42-1	IGHV4-39	IGHJ5	0.020067
10	IGHV4-39	IGHJ5	0.016722
15	IGHV1-69	IGHJ4	0.003413
20	IGHV1-69	IGHJ4	0.020619

Supplementary Table 5. Statistics for the pre-processing of the IGH NGS data

Sample	Raw read	UMI-processed read (functional filtering performed)	Unique consensus sequence #	Sampled UMI-processed read	Sampled unique consensus sequence #
A_d11	10,213,428	1,678,431	353,052	250,000	87,520
A_d17	4,718,128	404,665	100,031	250,000	69,541
A_d45	2,446,168	215,355	99,530	215,355	99,530
B_d10	3,918,963	148,132	45,698	148,132	45,698
B_d19	3,970,211	460,397	298,830	250,000	171,877
C_d6	4,206,074	538,240	310,825	250,000	157,012
C_d15	4,369,267	466,795	210,434	250,000	120,680
D_d6	4,308,679	457,369	160,539	250,000	103,612
D_d28	3,593,294	142,798	84,579	142,798	84,579
E_d23	4,937,896	782,329	262,323	250,000	104,363
E_d44	3,274,130	543,191	253,671	250,000	137,775
E_d99	3,900,483	276,160	58,633	250,000	54,760
F_d14	2,454,273	179,398	98,942	179,398	98,942
F_d36	2,060,695	187,156	142,352	187,156	142,352
G_d9	4,698,663	626,689	223,449	250,000	104,310
G_d22	3,577,375	529,997	296,335	250,000	155,254

Supplementary Table 6. Statistics for the pre-processing of the IGκ and IGλ NGS data

	Kappa chain (IGκ) repertoire			Lambda chain (IGλ) repertoire		
Sample	**Raw read**	**UMI-processed read (functional filtering performed)**	**Unique consensus sequence #**	**Raw read**	**UMI-processed read (functional filtering performed)**	**Unique consensus sequence #**
A_d11	1,147,464	8,354	2,662	2,085,248	36,557	6,826
A_d17	1,916,919	19,954	5,487	1,489,720	13,881	4,966
A_d45	1,315,147	46,260	19,151	1,496,933	72,241	22,959
B_d10	1,298,486	18,187	6,439	961,491	12,980	1,923
B_d19	1,223,146	25,509	11,159	3,590,964	357,920	56,717
C_d6	1,553,360	126,170	33,153	814,108	58,115	15,939
C_d15	1,508,906	158,103	29,785	925,777	37,942	6,198
D_d6	1,628,458	44,235	19,369	1,234,487	50,927	16,988
D_d28	1,189,263	81,625	25,463	1,022,841	92,332	21,447
E_d23	2,916,519	58,366	12,820	1,536,592	35,106	9,761
E_d44	1,634,121	64,292	19,155	1,543,971	139,647	26,723
E_d99	1,224,919	30,077	13,879	1,624,470	74,612	21,789
F_d14	1,439,098	8,848	2,555	1,035,486	7,955	3,644
F_d36	1,340,700	62,808	21,018	889,350	48,016	13,574
G_d9	2,265,376	16,048	4,147	1,310,891	8,694	4,571
G_d22	1,591,445	44,963	13,327	1,028,691	16,260	5,889

Supplementary Table 7. The RBD-binding predicted clones

Clone	HCDR1	HCDR2	HCDR3	V gene	J gene	Divergence	Mapped patient	Mapped isotype
P-003	GFYIH	RINPDSGATDYAQKFQG	GDLRD	IGHV1-2	IGHJ4	0.052863	E	A2
P-004	GYYMH	RINPNSGGTNYAQKFQG	GHMDV	IGHV1-2	IGHJ6	0.002212	A	G1
P-006	GYYMH	RINPNSGGTNYAQKFQG	RNMDV	IGHV1-2	IGHJ6	0.002963	A	G1
P-009	SNYMS	VIYSGGSTYYADSVKG	DAFGMDV	IGHV3-53	IGHJ6	0.006579	E	G1
P-014	SYSMN	YIYRRDSSIFYADSVKG	EDWQSLDY	IGHV3-48	IGHJ4	0.140969	A	A1
P-021	SYWIG	IIYPGDSDTRYSPSFQG	WDSRAFDI	IGHV5-51	IGHJ3	0	A	G1
P-022	TYWIG	IIYPGDSDTRYSPSFQG	YNSGWLDF	IGHV5-51	IGHJ4	0.013216	E	G1
P-023	SYGMH	VIWFDERNRYYSDSVKG	ANNYFPFDY	IGHV3-33	IGHJ4	0.034783	A	A1
P-026	SNYMS	VIYSGGSTYYADSVKG	DAQRYGMDV	IGHV3-53	IGHJ6	0.008772	E	A1
P-027	SNYMS	VLYSGGSTFYADSVKG	DAQVYGMDV	IGHV3-66	IGHJ6	0.013158	E	G1
P-031	SNYMS	VIYSGGSTYYADSVKG	DLAVYGMDV	IGHV3-53	IGHJ6	0.010965	A|E	G1
P-032	SNYMS	VIYSGGSTYYADSVKG	DLAVYGMDV	IGHV3-53	IGHJ6	0.010965	A|E	G1
P-035	SNYMT	VIYSGGSTFYADSVKG	DLGPGGMDV	IGHV3-53	IGHJ6	0.02193	E	G1
P-036	SNYMS	VIYSGGSTYYADSVKG	DLGPYGMDV	IGHV3-53	IGHJ6	0.008772	E	G1
P-042	SNYMN	VIYSGGSTYYADSVKG	DLPYYGMDV	IGHV3-66	IGHJ6	0.004386	E	G1
P-046	RNYMS	VIYSGGSTYYADTVKG	DLSAYGMDV	IGHV3-66	IGHJ6	0.013158	E	G1
P-047	SNYMN	VIYSGGSTFYADSVKG	DLSELGVDY	IGHV3-66	IGHJ4	0.008772	E	G2
P-048	SNYMN	VIYSGGSTFYADSVKG	DLSYYGMDV	IGHV3-53	IGHJ6	0.030702	A	G1
P-049	SNYMS	IIYSGGSTFYADSVKG	DLTIFGMDV	IGHV3-53	IGHJ6	0.017544	A	G1
P-050	SNYMS	VIYSGGSTYYADSVKG	DLTVYGMDV	IGHV3-53	IGHJ6	0.008772	E	A1
P-053	SNYMS	VIYAGGTTDYADSVKG	DLVAYGMDV	IGHV3-53	IGHJ6	0.039474	A	G1
P-055	DYYMS	YISSISSYTNYADSVKG	DLVGGAFDI	IGHV3-11	IGHJ3	0.004329	E	G1
P-056	SNYMS	VIYSGGSTFYADSVKG	DLVVLGMDV	IGHV3-66	IGHJ6	0.008772	E	A2
P-060	SNYMT	VIYSGGSTYYADSVKG	DLVVRGVDI	IGHV3-53	IGHJ3	0.013158	A	G1
P-061	SNYMS	LIYSGGSTYYADSVKG	DLVVSGMDV	IGHV3-66	IGHJ6	0.017544	E	A1
P-062	SNYMT	LIYSGGSTYYADSVKG	DLVVWGMDV	IGHV3-53	IGHJ6	0.039474	E	G1
P-063	SNYMT	VIYSGGSTYYADSVKG	DLVVYGMDV	IGHV3-53	IGHJ6	0.013158	E	A2
P-065	SNYMS	VLYSGGSTYYADSVKG	DLVYYGMDV	IGHV3-66	IGHJ6	0.013158	E	A1
P-068	SNYMS	VIYSGGSTFYADSVKG	DLYYYGMDV	IGHV3-53	IGHJ6	0.004386	A	G1
P-069	SNYMS	VIYSGGSTYYADSVKG	DLYYYGMDV	IGHV3-53	IGHJ6	0.000731	A	M|G1
P-070	SNYMS	IIYSGGSTFYADSVKG	DLYYYGMDV	IGHV3-53	IGHJ6	0.013158	A	G1
P-073	RNYMS	VIYSGGSTYYADSVKG	DVPIYGMDV	IGHV3-53	IGHJ6	0.013158	A	G1
P-074	SNYMS	VIYSGGSTDYADSVKG	DVVVYGMDV	IGHV3-53	IGHJ6	0.013158	E	A1
P-075	SNYMS	VIYSGGSTFYSDSVKG	DWGEYYFDY	IGHV3-66	IGHJ4	0.008772	E	A1
P-077	SNYMS	VIYSGGSTFYADSVKG	ELGVYGMDV	IGHV3-53	IGHJ6	0.013158	A	G1
P-078	SNYMS	VIYSGGSTFYADSVKG	ELYYYGMDV	IGHV3-53	IGHJ6	0.004386	A	G1
P-082	SNYMS	IIYSGGSTFYADSVKG	GYGDYYFDY	IGHV3-66	IGHJ4	0.013216	E	A1
P-085	SYWIG	IIYPGDSDTRYSPSFQG	QDSGWAFDY	IGHV5-51	IGHJ4	0.001087	A	G3|G1
P-087	SNYMS	LIYSGGSTFYADSVKG	SLEYYGMDV	IGHV3-53	IGHJ6	0.00885	E	G1
P-089	SNWIG	IIYPGDSDTRYSPSFQG	VGDGYPFDY	IGHV5-51	IGHJ4	0.008772	E	A1
P-090	SSNWWS	EIYHSGSTNYNPSLKS	VPQADAFDI	IGHV4-4	IGHJ3	0	A	G1
P-094	SYWIG	IIYPGDSDTRYSPSFQG	APATYASFDY	IGHV5-51	IGHJ4	0.013274	E	G1
P-095	SGDYYWS	YIYYSGSTYYNPSLKS	AQWLRGHHDY	IGHV4-30-4	IGHJ4	0.001431	A	G3|G1
P-100	SNYMS	VIYSGGSTYYADSVKG	DLDIVGAFDI	IGHV3-66	IGHJ3	0.002193	E	G1
P-104	SNYMS	VIYSGGSTYYADSVKG	DLDTAGGMDV	IGHV3-66	IGHJ6	0.02193	E	A1
P-111	SNYMN	VIYSGGTTYYADSVKG	DLEILGGMDV	IGHV3-53	IGHJ6	0.026316	A	G1
P-117	SNYMS	VIYSGGSTYYADSVKG	DLLEQGGMDV	IGHV3-66	IGHJ6	0.006579	E	G1
P-130	SNYMS	VIYSGGSTFYADSVKG	DLMAAGGMDV	IGHV3-53	IGHJ6	0.015351	A	G1
P-136	SNYMS	LIYSGGSTFYADSVKG	DLMAAGGMDV	IGHV3-53	IGHJ6	0.026316	A	G1
P-137	SNYMS	VIYSGGSTFYADSVKG	DLMAAGGMDV	IGHV3-53	IGHJ6	0.015351	A	G1
P-138	SNYMS	VIYSGGSRYYADSVKG	DLMAAGGMDV	IGHV3-53	IGHJ6	0.026316	A	G1
P-139	SNYMS	VIYSGGTTYYADSVKG	DLMAAGGMDV	IGHV3-53	IGHJ6	0.02193	A	G1
P-146	RNYMS	VIYSGGSTYYADFVKG	DLMAAGGMDV	IGHV3-53	IGHJ6	0.04386	A	G1
P-168	RNYMS	VIYSGGSTFYADSVKG	DLQEAGAFDI	IGHV3-53	IGHJ3	0.017544	A	A1
P-182	GYYMH	WINPNSGGTNYAQKFQG	DLSNVVFFDS	IGHV1-2	IGHJ4	0.004405	A	G1
P-186	SYWMS	NIKQDGSEKYYVDSVKG	DRWLRGDMDV	IGHV3-7	IGHJ6	0	A	G1
P-194	NAWMS	RIKTKTDGGTTDYAAPVKG	EWGYYDSLDY	IGHV3-15	IGHJ4	0.012658	E	G1
P-196	DYYMS	YISSSGSTIYYADSVKG	GEWLRGGFDP	IGHV3-11	IGHJ5	0	A	M|G3|G1
P-199	SYYMH	IIDPSGGSTSYAQKFQG	HDISPYYFDY	IGHV1-46	IGHJ4	0.004484	A	G1
P-201	SYWIG	IIYPGDSDTRYSPSFQG	HENLYYGMDV	IGHV5-51	IGHJ6	0	A	M|G1
P-207	SYWMS	NIKQDGSEKYYVDSVKG	HRWLRGEIDY	IGHV3-7	IGHJ4	0	E	G1
P-224	SSSYYWG	TFYYSRSTYYNPSLKS	LEWLRGHFDY	IGHV4-39	IGHJ4	0.012987	E	A1
P-230	SYWIG	IIYPGDSDTRYSPSFQG	MWSGVTAFDI	IGHV5-51	IGHJ3	0	E	M
P-231	SSSYYWG	SIYYSGSTYYNPSLKS	NEWLRGPFDY	IGHV4-39	IGHJ4	0.017316	A	G1
P-233	SYDIN	WMNPNSGNTGYAQKFQG	NPGGSGQFDP	IGHV1-8	IGHJ5	0.03125	A	M
P-234	RNYMS	VIYSGGSTFYADSVKG	PVMSRDGMDV	IGHV3-66	IGHJ6	0.011852	E	G1
P-235	SNYMS	VIYPGGTTYYADSVKG	QLPFGDYFDY	IGHV3-53	IGHJ4	0.030973	A	G1
P-242	SNFMS	VIYSGGSTYYADSVKG	QRWRQGWFDP	IGHV3-53	IGHJ5	0.004425	A	G1
P-243	SSSYYWG	SIYYSGSTYYNPSLKS	REWLRGHVDV	IGHV4-39	IGHJ6	0	E	G1

P-246	SSSYYWG	SIYYSGSTYYNPSLKS	RKWLRGAFDI	IGHV4-39	IGHJ3	0	E	G1
P-251	YYWIG	IIYPGDSDTRYSPSFQG	RSTTVGWLDY	IGHV5-51	IGHJ4	0.008734	E	G1
P-252	SYWMS	NIKQDGSEKYYVDSVKG	RVYYYGWLDV	IGHV3-7	IGHJ6	0.001456	A	G3|G1
P-261	SYGIH	LISYDGSDKYYADPVKG	SSWLRGAFDY	IGHV3-30	IGHJ4	0.038961	A	G1
P-268	SYYMH	IINPSGGSTSYAQKFQG	SSWYKLGFDP	IGHV1-46	IGHJ5	0	E	G1
P-269	SSSYYWG	SIYYSGSTYYNPSLKS	TPWLRGAFDY	IGHV4-39	IGHJ4	0.001082	E	G3|G1|A1
P-275	SYEMN	YISSSGSTIYYADSVKG	TQWLRGAFDI	IGHV3-48	IGHJ3	0	A	G1
P-315	VNYMT	LIYSGGSTYYADSVKG	VLPYGDYADF	IGHV3-53	IGHJ4	0.022026	E	A1
P-317	SNYMS	LIYSGGSTYYADSVKG	VLPYGDYVDY	IGHV3-53	IGHJ4	0.008811	A	G1
P-319	SNWIA	IIYPGDSDTTYSPSFQG	ALGHIGSGYDY	IGHV5-51	IGHJ4	0.04386	E	G1
P-320	SHWIG	IIYPGDSDTRYSPSFQG	APSGYYNWFDP	IGHV5-51	IGHJ5	0.008772	A	G1
P-321	SYGMH	IISYDGSNKYYADSVKG	AQSWLHWYFDL	IGHV3-30	IGHJ2	0.004348	E	G1
P-322	HYAIS	RIIPMLDISNYAQKFKG	DHTILPKGMDV	IGHV1-69	IGHJ6	0.044053	E	G2
P-324	DYAMS	FIRSKAYGGTTEYAASVKG	DLRGSSGWYDI	IGHV3-49	IGHJ3	0.004219	E	A2
P-326	SYAMH	VISSDGGNKYYADSVKG	DTLLLVDAFDI	IGHV3-30-3	IGHJ3	0.008658	A	G1
P-327	DYQMS	YISSSSSYTNYADSVKG	DWGYSSPRFDY	IGHV3-11	IGHJ4	0.008658	E	G1
P-331	SYWIG	IIYPGDSDTRYSPSFQG	HGNWANSDLDY	IGHV5-51	IGHJ4	0.015217	A	G1
P-333	SYWIA	IIYPGDSDTRYSPSFQG	LPSSWYNWFDP	IGHV5-51	IGHJ5	0.0131	E	G1
P-335	SDWIG	IIYPGDSDTRYSPSFQG	MLCGGDCPFDY	IGHV5-51	IGHJ4	0.00885	E	A1
P-338	SYWIG	IIYPGDSDTRYSPSFQG	SIVTTNAGFDF	IGHV5-51	IGHJ4	0.008811	E	G1
P-340	SYWIG	IIYPGDSDTRYSPSFQG	SSSGPHDAFDI	IGHV5-51	IGHJ3	0	E	M
P-341	SNYMS	VIYSGGSTFYADSVKG	VLPLYGDYLDY	IGHV3-53	IGHJ4	0.004405	E	A1
P-342	SYGIT	WISAYNGNTKYAQKLQG	VMGIAVAGTVV	IGHV1-18	IGHJ6	0.015487	A	G1
P-345	SYAMH	AISSNGGSTYYANSVKG	VPDDLIWYFDL	IGHV3-64	IGHJ2	0.001449	E	G3|G1
P-346	SYAMH	AISSNGGSTYYANSVKG	VPDDLNWYFDL	IGHV3-64	IGHJ2	0.002899	E	G1
P-348	SYGIS	WISAYNGNTNYAQKLQG	VVELGIGWFDP	IGHV1-18	IGHJ5	0	A	G1
P-349	STSFHWG	TISYSGRAYHNPSLKS	WNSHYYYGMHV	IGHV4-39	IGHJ6	0.081897	A	G2
P-353	SYWIA	IIYPGDSDTRYSPSFQG	YSSSPNGWFDP	IGHV5-51	IGHJ5	0.006579	E	G1
P-357	NYAMS	AISGSGGSTYYADSVKG	AIAAAGYWVFDY	IGHV3-23	IGHJ4	0.004386	E	G1
P-358	KCVMS	SISDGGDNINDADSVKG	AKSGSDRHVFEI	IGHV3-23	IGHJ3	0.104348	A	G2
P-362	SVDYYWS	YIYYSGSTYYNPSLKS	DLRWGRGGGMDV	IGHV4-30-4	IGHJ6	0.029915	A	G1
P-363	DYAMH	GISWNSGNIGYADSVKG	DSLGELLSGMDV	IGHV3-9	IGHJ6	0.004292	E	G1
P-365	DYAMH	GISWNSGSIGYADSVKG	DSSAGHGDYFDY	IGHV3-9	IGHJ4	0.004329	A	G1
P-366	DYAMH	GISWNSGGIAYADSVKG	DSSAGHGDYFDY	IGHV3-9	IGHJ4	0.008658	A	G1
P-369	SNAIS	RIIPIFGTANYAQKFQG	DVIESPLYGMDV	IGHV1-69	IGHJ6	0.030837	A	G1
P-382	SFAIT	RIIPILGIANYAQKFQG	EFSGGDNTGFDY	IGHV1-69	IGHJ4	0.008811	E	G1
P-385	RNYMS	VIYSGGTTYYTDSVKG	GDILTAPPPIDY	IGHV3-66	IGHJ4	0.017621	E	A1
P-387	SNIVTWI	RTYYRSKWYNDYAVSVKS	GRFGGYFYGMDV	IGHV6-1	IGHJ6	0.064655	A	G2
P-388	DYAMH	GISWNSGSIGYADSVKG	GRLGELLDAFDI	IGHV3-9	IGHJ3	0	A	M|G1
P-389	SYWMH	RINGDGSDTGYADSLRA	GVDYGRGAVLQH	IGHV3-74	IGHJ1	0.073913	A	A2
P-392	DYWIG	IIYPGDSDTRYSPSFQG	HSLADPVHWFDP	IGHV5-51	IGHJ5	0.017391	E	A1
P-394	SYWIG	IIYPGDSDTRYSPSFQG	LESIAAAGWADY	IGHV5-51	IGHJ4	0	E	A1
P-395	SYWIG	IINPGDSETIYSPSFQG	LGSGGSHNWFDP	IGHV5-51	IGHJ5	0.017467	E	G1
P-398	SGDYYWN	YIYYSGSTYYNPSLKS	SSPLVVTDAFDI	IGHV4-30-4	IGHJ3	0.006579	A	G1
P-400	SNFMS	VIYSGGSTYYADSVKG	VGWGYDSEYFDL	IGHV3-53	IGHJ2	0.024229	E	A1|A2
P-404	SNSAAWN	RTYYRFKWYYDYALSLES	VSAPGPRGWFDP	IGHV6-1	IGHJ5	0.050633	E	G1
P-406	SNYMS	LIYSGGSTYYADSVKG	ALEVNAFGDYFDY	IGHV3-66	IGHJ4	0.004405	E	A1
P-408	SYYMH	IINPGGGSTSYAQKFQG	DAGYVPTTGGMDV	IGHV1-46	IGHJ6	0.017621	E	G1
P-409	TYYWS	YIYNSGSTNYNPSLKS	DANLSGSFDALDI	IGHV4-59	IGHJ3	0.061404	E	G1
P-410	DYAMH	GISWNSGTIGYADSVKG	DGGAVAETYGMDV	IGHV3-9	IGHJ6	0.008621	E	G1
P-411	SHYMH	IINPSGGSTSYAQKFQG	DGYFVPARSAFDI	IGHV1-46	IGHJ3	0.008811	E	M
P-435	SYYMH	IINPDAGSTTYAQKFQG	DLYGLPGRAAFDI	IGHV1-46	IGHJ3	0.022026	A	G1
P-440	NHYMH	IINPSGGSTSYAQKFQG	DRWFIPQSGYFDL	IGHV1-46	IGHJ2	0.011013	A	G1
P-441	SYYMH	IINPSGGSTSYAQKFQG	DSYYLPAMGPFDY	IGHV1-46	IGHJ4	0	A	G1
P-447	SYYMH	IINPSGGSTSYAQKFQG	GAWGVPAASPSDP	IGHV1-46	IGHJ5	0	E	G1
P-448	SNYMS	VIYSGGSTYYADSVKG	GDGSGDYYYGMDV	IGHV3-53	IGHJ6	0	E	A2
P-449	SNYMS	VIYSGGSTFYADSVKG	GDGSGDYYYGMDV	IGHV3-53	IGHJ6	0.008811	E	A2
P-453	SYYMH	IINPSGGSTSYAQKFQA	GGVVPAASSAFDI	IGHV1-46	IGHJ3	0.017699	E	G1
P-454	SYAMH	VISYDGSNKYYADSVKG	GKWYSSPLEYFDY	IGHV3-30-3	IGHJ4	0.008621	A	G1
P-455	DYAMH	AISWNSGSIDYADSVKG	GLLAEFVVPTLDY	IGHV3-9	IGHJ4	0.008696	E	A1
P-456	SYWIS	RIDPSDSYTNYSPSFQG	GQQWLSNNWYFDL	IGHV5-10-1	IGHJ2	0.001096	E	M|G3|G1
P-458	SYWIG	IIYPGDSDTRYSPSFQG	HLDWNAPRGAFDI	IGHV5-51	IGHJ3	0	A	G1
P-461	SYWIG	IIYPGDSDTRYSPSFQG	HLDWNAPRGPFDI	IGHV5-51	IGHJ3	0	A	G1
P-468	SSNWWS	EIYHSGSTNYNPSLKS	LGHGDPGLRYFDL	IGHV4-4	IGHJ2	0	E	G1
P-472	SSNWWS	EIFHSGSASYNPSLKS	LGHGDPGLRYFDL	IGHV4-4	IGHJ2	0.022026	E	A1
P-475	NAWMS	RIKSKTDGGTTDYAAPVKG	NDVIQYYHYGMDV	IGHV3-15	IGHJ6	0.004348	A	G1
P-476	NAWMS	RIKSKTDGGTTDYAAPVKG	NDVLQYYYYGMDV	IGHV3-15	IGHJ6	0	A	G1
P-477	DFAMS	FIRGTAYGGTTEYAASVKG	NHMTTVTWLGADI	IGHV3-49	IGHJ3	0.013043	E	G1
P-481	GYYMH	RINPNSGGTNYAQKFQG	PGSISLVRGVRDV	IGHV1-2	IGHJ6	0	E	G3
P-483	NAWMS	RIKSKTDGGTTDYAAPVKG	SDILQYYYYGMDV	IGHV3-15	IGHJ6	0.002128	E	M
P-485	NYGMH	GVSYDGSDKYYADSVKG	TVATHYYYYGMDV	IGHV3-30	IGHJ6	0.030303	E	G3
P-487	SYAIS	RIIPILGIANYAQKFQG	AALYGDYEEGYFDY	IGHV1-69	IGHJ4	0	E	G1
P-488	SYGMH	VISYDGSNKYYADSVKG	AGYSYGYPEIYFDY	IGHV3-30	IGHJ4	0.006522	E	G1
P-489	DYAMH	GISWNSGTIGYADSVKG	ALQPMDGGEYYFDY	IGHV3-9	IGHJ4	0.004348	E	A1

P-491	DYAMY	GSSWNSGTIGYADSVKG	DAGVTEYYYYGMDV	IGHV3-9	IGHJ6	0.034483	A	G1
P-499	DYAMH	GISWNSGTIGYADSVKG	DIGFGELLSYGMDV	IGHV3-9	IGHJ6	0.004292	A	M
P-500	DYAMH	GISWNSGTIGYADSVKG	DIRKGDGFEFYFDY	IGHV3-9	IGHJ4	0.008584	E	A2
P-506	DYAMH	GSSWNSGTIGYADSVKG	DMGRGNDNNLAFDI	IGHV3-9	IGHJ3	0.038961	E	G1
P-507	SYAMS	AISGSGGSTYYADSVKG	DPMVRGPSFDYFDY	IGHV3-23	IGHJ4	0	A	G3|G1|A1
P-511	RYGMH	VISYDGSNKYYVDSVKG	DVPLGIAATYLFDY	IGHV3-33	IGHJ4	0.017316	E	G1
P-512	SNYMS	VIYSGGSTFYADSVKG	EAGMGAAAGTAFDY	IGHV3-53	IGHJ4	0.004386	E	G1
P-513	SYYMH	IINPSGGSTSYAQKFQG	EGVWDSSGYSSFDY	IGHV1-46	IGHJ4	0.013216	E	A1
P-524	DYAMH	GISWNSGSIVYADSVKG	GHTAMHYYYYGMDV	IGHV3-9	IGHJ6	0.008696	E	G1
P-526	SYWIG	IIYPGDSDTRYSPSFQG	HEGACSGGSCGIDY	IGHV5-51	IGHJ4	0	A	G1
P-529	NYGMH	VISYDGSNKYYADSVKG	NIYSYAYPQYYFDY	IGHV3-30	IGHJ4	0.021645	A	G1
P-533	NYGMH	GVSYDGSDKYYADSVKG	TVATHYYYYYGMDV	IGHV3-30	IGHJ6	0.030303	E	G3
P-547	SYWIG	IIYPGDSDTRYSPSFQG	AGDSSGWAPLDAFDI	IGHV5-51	IGHJ3	0.013274	A	G1
P-548	SYGMH	VISYDGSNKYYADSVKG	APIGYCTNGVCYFDY	IGHV3-30	IGHJ4	0	A	M|G1
P-550	SYAIS	RIIPILGIANFIANYAQKFQG	DDYSNYDYYYYGMDV	IGHV1-69	IGHJ6	0.050209	E	A1
P-561	DYAMH	GVTWNSGSIGYADSVKG	DISPMLRGDNYGMDV	IGHV3-9	IGHJ6	0.017167	E	G1
P-591	SNYMS	VIYSGGSTYYADSVKG	DLRDSSGYSFGAFDI	IGHV3-53	IGHJ3	0	E	A1
P-592	SYGMH	FISYDGSNKYYADSVKG	DMAVAGYYYYYGMDV	IGHV3-33	IGHJ6	0.008658	E	G1
P-610	SYYMH	IINPSGGSRSYAQKFQG	DYDYVWGSYPNAFDI	IGHV1-46	IGHJ3	0.008811	A	G1
P-611	SYYMH	IINPSGGSTSYAQKFQG	DYDYVWGSYPNAFDI	IGHV1-46	IGHJ3	0	A	G1
P-614	SYAIS	GIIPMFGTANYAQKFQG	ERSVTKNLYYYGMDV	IGHV1-69	IGHJ6	0.004405	A	G1
P-616	SYAIS	GIIPIFGTANYAQKFQG	FPTYHDILTGYEVDY	IGHV1-69	IGHJ4	0	E	G1
P-621	SYAIS	RIIPILGIANYAQKFQG	GIGYSGSGSNDYFDS	IGHV1-69	IGHJ4	0.002212	E	G1
P-629	NYAIS	RIIPILGIANYAQKFQG	GIGYSGSGSNDYFDY	IGHV1-69	IGHJ4	0.004425	E	G3
P-631	SYGMH	VISYDGSNEYYADSVKG	GPWYSSGWYYQGFED	IGHV3-33	IGHJ4	0.004348	E	G3
P-634	SYAIS	RIIPMFGIANYAQKFQG	HKYEYYDSSGYPFDY	IGHV1-69	IGHJ4	0.011111	E	G1
P-637	SYWIG	IIYPGDSDTRYSPSFQG	LHRPYGDLQYNWFDP	IGHV5-51	IGHJ5	0.0131	E	G1
P-640	SYWIG	IIYPGDSDTRYSPSFQG	PPNSSGANFRNAFDI	IGHV5-51	IGHJ3	0	A	G1
P-641	GYYMH	WINPNSGGTNYAQKFQG	PPPTVTHYYYYGMDV	IGHV1-2	IGHJ6	0	A	G1|G2
P-649	NAWMS	RIKSKTDGGTTDYAAPVKG	AGRTKRNYYYYYGMDV	IGHV3-15	IGHJ6	0	E	G1
P-651	SYAIS	GIIPIFGTANYAQKFQG	DHRILSAGYYYYGMDV	IGHV1-69	IGHJ6	0	E	A2
P-653	DYAMH	GITWNSGSIGYADSVKG	DIGPYDFWSRSYGMDV	IGHV3-9	IGHJ6	0.00431	A	G1
P-659	SYATH	VISSDGSKKYYADSVKG	DLVPWLVVKFHYGVDV	IGHV3-30	IGHJ6	0.069869	E	G2|A2
P-662	DYAMH	GISWNSGSIGYADSVKG	DRAVREGYNYYYGMDV	IGHV3-9	IGHJ6	0	A	G1
P-663	TYAMS	AISGSGGNTYYADSVKG	DRWRESSGWYPDAFDI	IGHV3-23	IGHJ3	0.017316	E	G1
P-666	SYWMS	NIKQDGSEKYYVDSVKG	DVRYDSSGYYDIFRDY	IGHV3-7	IGHJ4	0.002597	A	G1
P-667	NHAMY	VISYDGSKEYYADSVKG	EEGGSYFTHYYYGMDV	IGHV3-30-3	IGHJ6	0.034632	A	G1
P-668	SYAIS	GIIPIFGTANYAQKFQG	GGATYCSGGSCYSFDH	IGHV1-69	IGHJ4	0.00885	E	G1
P-669	SYAIS	GIIPIFGTANYAQKFQG	GGATYCSGGSCYSFDY	IGHV1-69	IGHJ4	0.004425	E	G1
P-670	DYAMH	GSSWNSGSIGYADSVKG	GKSPLDYDQTMGAFDI	IGHV3-9	IGHJ3	0.013043	E	A1
P-678	DYAMH	GSSWNSGSIGYADSVKG	GKSPLDYDQTMGAFDI	IGHV3-9	IGHJ3	0.013043	E	A1
P-679	DYAMH	GISWNSGFMGYADSVKG	GLYQVRYKYYYYALDV	IGHV3-9	IGHJ6	0.106667	A	A1
P-680	SYWIG	IIYPGDSDTRYSPSFQG	HNTIFGVLGSDYGMDV	IGHV5-51	IGHJ6	0	E	A1
P-681	SHWIS	RIDPSDSYTNYSPSFQG	HTLLGELSSPTNWFDP	IGHV5-10-1	IGHJ5	0.017544	E	G1
P-683	SSSYYWG	SIYYSGSTYYNPSLKS	RVRQWLVRPSWAAFDI	IGHV4-39	IGHJ3	0	E	A1
P-688	DYAMS	FIRSKAYGGTTEYAASVKG	VDGLSSGSYLLPSIDY	IGHV3-49	IGHJ4	0.002119	E	G1
P-690	GYYMH	WINPNSGGTNYAQKFQG	VPYYYDSSGHRGGMDV	IGHV1-2	IGHJ6	0.00177	A	M|G3|G1
P-697	SYGIS	WISAYNGNTNYAQKLQG	DRPDYDYVWGSLVPFDY	IGHV1-18	IGHJ4	0.013216	A	G1
P-698	GYYMH	RINPNSGGTNYAQKFQG	DYYASGSYSPEDYGMDV	IGHV1-2	IGHJ6	0	A	G1
P-701	GYYMH	RINPNSGGTNYAQKFQG	DYYASGSYSPEDYGMDV	IGHV1-2	IGHJ6	0	A	G1
P-702	DYAMH	GISWNSGRIGYADSVKG	EGTGDGYNLLIGGAFDI	IGHV3-9	IGHJ3	0.017316	A	G1
P-705	TYGMH	VISYDGSNKYYADSVKG	GAFYYYGSGSYHYGMDV	IGHV3-30	IGHJ6	0.004348	A	G1
P-708	SYAIS	GIIPIFGTANYAQKFQG	PEWDYGDPLGYYYGMDV	IGHV1-69	IGHJ6	0.002232	A	G1
P-712	SYSMN	SISSSSSYIYYADSVKG	VPAMEDGDYYYYYGMDV	IGHV3-21	IGHJ6	0	E	G2
P-714	RYAIS	RIIPILGIANYAQKFQG	YDFWSGQNTNYYYVLDV	IGHV1-69	IGHJ6	0.004505	E	G1
P-716	DYAMS	FIRSKAYGGTTEYAASVKG	DEDSGTLLPGFYYYDMDV	IGHV3-49	IGHJ6	0	A	G1
P-722	DYAMS	FIRSKAYGGTTEYAASVKG	DEDSGTLLPGFYYYGMDV	IGHV3-49	IGHJ6	0.004219	A	M|G1

P-724	SYYMH	IINPSGGSTSYSQKFQG	DGIAAAGTEYYYYYGMDV	IGHV1-46	IGHJ6	0.008811	A	G1
P-726	SYYMH	IINPSGGSTSYAQKFQG	DGIAAGGTEYYYYYGMDV	IGHV1-46	IGHJ6	0.004405	A	G1
P-731	SYGMH	VISYDGSNKYYADSVKG	DITFDWLGVWYYYYGMDV	IGHV3-30	IGHJ6	0	A	G3
P-735	SYAIS	GIIPIFGTANYAQKFQG	EKAVAGPRPSYYYYGMDV	IGHV1-69	IGHJ6	0	E	G1
P-736	SGNYYWS	YIYYSGSTNYNPSLKS	ETYYYDSSGYYGSDAFDI	IGHV4-61	IGHJ3	0.017094	A	G1
P-739	TYWIN	RIDPSDSYTNYSPSFQG	GDYYDNSDYSGLSEYFQH	IGHV5-10-1	IGHJ1	0.015351	E	G1
P-760	SYWMS	NIEQDGSEKYYVDSVKG	IYGYYDRSGYYYGEYFQH	IGHV3-7	IGHJ1	0.008734	E	G1
P-761	GYYMH	WINPNSGGTNYAQKFQG	LPFPYYYDSSGYYAAFDI	IGHV1-2	IGHJ3	0	A	G1
P-762	DYAMS	FIRGKAYGGTSEYAASVKG	NIALVVYGMRLDYYGMDV	IGHV3-49	IGHJ6	0.025532	A	G1
P-765	SYAIS	GIIPMFGTANYAQKFQG	RIVVVPAGPWFYYYGMDV	IGHV1-69	IGHJ6	0.008969	A	G1
P-771	RYAMH	WINAGNGKTKYSQKFQG	ALYYYDSSGSTQSDDAFDI	IGHV1-3	IGHJ3	0.00885	E	G1
P-773	RYAMH	WINAGNGNTKYSQKFQG	ALYYYDSSGSTQSDDAFDI	IGHV1-3	IGHJ3	0.013274	E	G1
P-791	SNYMS	VIYSGGSTYYADSVKG	DGQRMAAAGTEDYYYGMDV	IGHV3-66	IGHJ6	0.001096	E	G1|A1|A2
P-796	SNYMS	VIYSGGSTYYADSVKG	DGQRMAAAGTEDYYYGMDV	IGHV3-66	IGHJ6	0.001096	E	G1|A1|A2
P-810	DYAMH	GISWNSGTIGYADSVKG	DTGMRYSSGWYGDDYGMDV	IGHV3-9	IGHJ6	0.004329	A	G1
P-819	SYAIS	GIIPIFGTANYAQKFQG	ERRCGDCYEPHYYYYGMDV	IGHV1-69	IGHJ6	0	E	A1
P-829	SYGMH	VISYDGSNKYYADSVKG	VLADYGDYHVSLGYYGMDV	IGHV3-30	IGHJ6	0	A	G1
P-830	SYGIS	WISAYNGNTNYAQKLQG	VLYYYDRSGYYSSESDFQH	IGHV1-18	IGHJ1	0	A	G1
P-833	DYAMH	GISWNSGTIGYADSVKG	AGGPLDGSGSYSQPEYYFDY	IGHV3-9	IGHJ4	0.004348	E	A2
P-835	SYGMH	VISYDGSNKYYADSVKG	ATQRLYYYASGSFLPDAFDI	IGHV3-30	IGHJ3	0	E	G1
P-837	TYGMH	VISYDGSNKYYADSVKG	ATQRLYYYGSGSYLPDAFDI	IGHV3-30	IGHJ3	0.005797	E	G1
P-839	DYAMH	GISWNSGTIGYADSVKG	DENRGYSSRWYDPEYYGMDV	IGHV3-9	IGHJ6	0.004329	A	G1
P-841	DYAMH	GISWNSGTIGYADSVKG	DENRGYSSSWYDPEYYGMDV	IGHV3-9	IGHJ6	0.006494	A	G1
P-842	DYAMH	GITWNSGSIGYADSVKG	DENRGYSSSWYDPEYYGMDV	IGHV3-9	IGHJ6	0.008658	A	G1
P-845	DYAMH	GISWNSGTIGYADSVKG	DIGPEGGYSWRRGVYYGMDV	IGHV3-9	IGHJ6	0.008584	A	G1
P-846	DYAMH	GISWNSGTIGYADSVKG	DISTYYGSGSYYDEDYGMDV	IGHV3-9	IGHJ6	0.012876	E	G1
P-847	DYAMH	GISWNSGTIGYADSVKG	DVPTYYYDSSGWAEHYGMDV	IGHV3-9	IGHJ6	0.00431	A	G1
P-851	SYSIT	RIIPILGIANFAQKFQG	ESGGHYYGSGSYYNSNWFDP	IGHV1-69	IGHJ5	0.013216	E	A1
P-858	SYSMN	SISSSSSYIYYADSVKG	VGEGPTVAQDDYYYYYDMDV	IGHV3-21	IGHJ6	0	E	G1|A1
P-859	SYGIS	WISAYNGNTNYAQKLQG	VSFYYDSSGYYSANGNGMDV	IGHV1-18	IGHJ6	0	E	G1
P-867	DYGMS	GINWNGGNTGYADSVKG	AAEGKLRYFDWLFFADYGMDV	IGHV3-20	IGHJ6	0.01087	E	G1
P-868	SYAMS	AISGSGGSTYYADSVKG	ANGYCSSTSCLDYYYYGMDV	IGHV3-23	IGHJ6	0	E	G1
P-875	NAWMS	RIKSKTDGGTTDYAAPVKG	DKAGYCSSTSCYARELDAFDI	IGHV3-15	IGHJ3	0	E	M|G1|A2
P-878	NAWMS	RIKSKTDGGTTDYAAPVKG	DKAGYCSSTSCYARELDAFDI	IGHV3-15	IGHJ3	0	E	M|G1|A2
P-890	RYAIS	GIIPIFGTANYAQKFQG	ERTYCSSTSCYAGYYYYGMDV	IGHV1-69	IGHJ6	0.004405	A	G1|A1
P-892	RYAIS	GIIPIFGTANYAQKFQD	ERTYCSSTSCYAGYYYYGMDV	IGHV1-69	IGHJ6	0.017621	A	G1
P-911	RYAIS	GIIPIFGTANYAQKFQG	ERTYCSSTSCYAGYYYYGMDV	IGHV1-69	IGHJ6	0.004405	A	G1|A1
P-912	RYAIS	GIIPIFGTANYAQKFQD	ERTYCSSTSCYAGYYYYGMDV	IGHV1-69	IGHJ6	0.017621	A	G1

P-919	DYAMH	GISWNSGTIGYADSVKG	DIAPHYYDILTGYYEGAWGFDY	IGHV3-9	IGHJ4	0.012876	A	G1
P-920	SYGMH	VISSDGSNKYYADSVKG	DLGVVPAASRWDDYYYYYGMDV	IGHV3-30	IGHJ6	0.010823	E	G1
P-922	SYGIS	WISAYNGNTNYAQKLQG	DRENLSIFGVSQRLTRYYGMDV	IGHV1-18	IGHJ6	0.008811	E	G1
P-924	SYAIS	GIIPIFGTANYAQKFKG	EEFDLVVVPAATTQYYYYGMDV	IGHV1-69	IGHJ6	0.004405	A	G1
P-926	TSGVGVG	LIYWDDDKRYSPSLKS	SPDRRYYDILTGYSNLYWYFDL	IGHV2-5	IGHJ2	0	A	M
P-929	SYAMS	AISGSGGSTYYADSVKG	ALYDSSGYYRPGRDFYYYYAMDV	IGHV3-23	IGHJ6	0	A	G1
P-930	DYAMH	GISWNSGTIGYADSVKG	DIKKLYYDILTGYYNDADYGMDV	IGHV3-9	IGHJ6	0.004292	A	G3
P-932	DYAMH	GISWNSGVIGYADSVKG	DIKRFYYDILTGYYNDADYGMDV	IGHV3-9	IGHJ6	0.008584	A	G3
P-935	NAWMS	RIKSKTDGGTTDYAAPVKG	DVSGGYYGSGGYYKYYYYYGMDV	IGHV3-15	IGHJ6	0	A	G3
P-937	DYYIH	RINPNSGGTNYAQKFQG	EGGEWYDSSGYYSTWSYYYGMDV	IGHV1-2	IGHJ6	0.008811	E	G1
P-939	SYWMS	NIKQDGSEKYYVDSVKG	EGGPNYYDSSGYYYDSYYYGMDV	IGHV3-7	IGHJ6	0	A	G1
P-940	SYWMS	NIKQDGSEKYYVDSVKG	EGGPNYYDSSGYYYDYYYYGMDV	IGHV3-7	IGHJ6	0.004329	A	G1
P-941	SYWIG	IIYPGDSDTRYSPSFQG	HPPDYYGSGSYYNGGPGMGGMDV	IGHV5-51	IGHJ6	0.002174	A	M|G1
P-945	SYAIS	GIIPIFGTANYAQKFQG	VAERVHYDILTGYYPYYYYAMDV	IGHV1-69	IGHJ6	0.00885	E	G1

Supplementary Table 8. Primers used in the study

Primers used for the amplification of antibody gene

Name	Sequence	Step
IgM-RT	TGACTGGAGTTCAGACGTGTGCTCTTCCGATCTNNNNTNNNNTNNNNGAAGGAAGTCCTGTGCGAG	RT
IgG-RT	TGACTGGAGTTCAGACGTGTGCTCTTCCGATCTNNNNTNNNNTNNNNGGGAAGTAGTCCTTGACCA	RT
IgA-RT	TGACTGGAGTTCAGACGTGTGCTCTTCCGATCTNNNNTNNNNTNNNNGGGGAAGAAGCCCTGGAC	RT
IgD-RT	TGACTGGAGTTCAGACGTGTGCTCTTCCGATCTNNNNTNNNNTNNNNTGGGTGGTACCCAGTTATCAA	RT
IgE-RT	TGACTGGAGTTCAGACGTGTGCTCTTCCGATCTNNNNTNNNNTNNNNAAGTAGCCCGTGGCCAGG	RT
VH1	ACACTCTTTCCCTACACGACGCTCTTCCGATCTGGCCTCAGTGAAGGTCTCCTGCAAG	2nd strand synthesis
VH2	ACACTCTTTCCCTACACGACGCTCTTCCGATCTGTCTGGTCCTACGCTGGTGAACCC	2nd strand synthesis
VH3	ACACTCTTTCCCTACACGACGCTCTTCCGATCTCTGGGGGGTCCCTGAGACTCTCCTG	2nd strand synthesis
VH4	ACACTCTTTCCCTACACGACGCTCTTCCGATCTCTTCGGAGACCCTGTCCCTCACCTG	2nd strand synthesis
VH5	ACACTCTTTCCCTACACGACGCTCTTCCGATCTCGGGGAGTCTCTGAAGATCTCCTGT	2nd strand synthesis
VH6	ACACTCTTTCCCTACACGACGCTCTTCCGATCTTCGCAGACCCTCTCACTCACCTGTG	2nd strand synthesis
LC-RT	CACCAGTGTGGCCTTGTTGGCTTG	RT
KC-RT	GTTTCTCGTAGTCTGCTTTGCTCA	RT
VK1-fwd	ACACTCTTTCCCTACACGACGCTCTTCCGATCTATGAGGGTCCCCGCTCAGCTGCTGG	First round of PCR
VK2-fwd	ACACTCTTTCCCTACACGACGCTCTTCCGATCTATGAGGCTCCCCGCTCAGCTGCTGG	First round of PCR
VK3-fwd	ACACTCTTTCCCTACACGACGCTCTTCCGATCTATGAGGGTCCCTGCTCAGCTGCTGG	First round of PCR
VK4-fwd	ACACTCTTTCCCTACACGACGCTCTTCCGATCTATGAGGCTCCCTGCTCAGCTGCTGG	First round of PCR
VK5-fwd	ACACTCTTTCCCTACACGACGCTCTTCCGATCTCTCTTCCTCCTGCTACTCTGGCTCCCAG	First round of PCR
VK6-fwd	ACACTCTTTCCCTACACGACGCTCTTCCGATCTATTTCTCTGTTGCTCTGGATCTCTG	First round of PCR
VK7-fwd	ACACTCTTTCCCTACACGACGCTCTTCCGATCTAGCTCCTGGGGCTCCTGCTGCTCTG	First round of PCR
VK8-fwd	ACACTCTTTCCCTACACGACGCTCTTCCGATCTATGAGGCTCCCTGCTCAGCTCTTGG	First round of PCR
VK9-fwd	ACACTCTTTCCCTACACGACGCTCTTCCGATCTATGGGGTCCCAGGTTCACCTCCTC	First round of PCR
VK10-fwd	ACACTCTTTCCCTACACGACGCTCTTCCGATCTATGTTGCCATCACAACTCATTGGG	First round of PCR
VK1-rev	TGACTGGAGTTCAGACGTGTGCTCTTCCGATCTNNNNTNNNNTNNNNTTTGATATCCACCTTGGTCCC	First round of PCR
VK2-rev	TGACTGGAGTTCAGACGTGTGCTCTTCCGATCTNNNNTNNNNTNNNNTTTAATCTCCAGTCGTGTCCC	First round of PCR
VK3-rev	TGACTGGAGTTCAGACGTGTGCTCTTCCGATCTNNNNTNNNNTNNNNTGATCTCCAGCTTGGTCCCC	First round of PCR
VL1-fwd	ACACTCTTTCCCTACACGACGCTCTTCCGATCTGGTCCTGGGCCCAGTCTGTGCTG	First round of PCR
VL2-fwd	ACACTCTTTCCCTACACGACGCTCTTCCGATCTGGTCCTGGGCCCAGTCTGCCCTG	First round of PCR
VL3-fwd	ACACTCTTTCCCTACACGACGCTCTTCCGATCTGCTCTGTGACCTCCTATGAGCTG	First round of PCR
VL4-fwd	ACACTCTTTCCCTACACGACGCTCTTCCGATCTGGTCTCTCTCGCAGCCTGTGCTG	First round of PCR
VL5-fwd	ACACTCTTTCCCTACACGACGCTCTTCCGATCTGGTCTCTCTCCCAGCCTGTGCTG	First round of PCR
VL6-fwd	ACACTCTTTCCCTACACGACGCTCTTCCGATCTGGTCTCTCTCGCAGCTTGTGCTG	First round of PCR
VL7-fwd	ACACTCTTTCCCTACACGACGCTCTTCCGATCTGGTCTCTCTCCCAGCTTGTGCTG	First round of PCR
VL8-fwd	ACACTCTTTCCCTACACGACGCTCTTCCGATCTGTTCTTGGGCCAATTTTATGCTG	First round of PCR
VL9-fwd	ACACTCTTTCCCTACACGACGCTCTTCCGATCTGGTCCAATTCCCAGGCTGTGGTG	First round of PCR
VL10-fwd	ACACTCTTTCCCTACACGACGCTCTTCCGATCTGGTCCAATTCTCAGGCTGTGGTG	First round of PCR
VL11-fwd	ACACTCTTTCCCTACACGACGCTCTTCCGATCTGAGTGGATTCTCAGACTGTGGTG	First round of PCR
VL12-fwd	ACACTCTTTCCCTACACGACGCTCTTCCGATCTGGTCCTGGGCCCAGTCTGTCGTG	First round of PCR
VL13-fwd	ACACTCTTTCCCTACACGACGCTCTTCCGATCTAGTGTCAGTGGTCCAGGCAGGGC	First round of PCR
VL14-fwd	ACACTCTTTCCCTACACGACGCTCTTCCGATCTACAGGATCCTGGGCTCAGTCTGC	First round of PCR
VL15-fwd	ACACTCTTTCCCTACACGACGCTCTTCCGATCTCTCCTATGAGCTGACTCAGCCAC	First round of PCR
VL16-fwd	ACACTCTTTCCCTACACGACGCTCTTCCGATCTTCTTCTGAGCTGACTCAGGACCC	First round of PCR
VL17-fwd	ACACTCTTTCCCTACACGACGCTCTTCCGATCTAGGTCTCTGTGCTCTGCCTGTGC	First round of PCR
VL18-fwd	ACACTCTTTCCCTACACGACGCTCTTCCGATCTAGGTTCCCTCTCGCAGCCTGTGC	First round of PCR
VL1-rev	TGACTGGAGTTCAGACGTGTGCTCTTCCGATCTNNNNTNNNNTNNNNAGGACGGTGACCTTGGTCCC	First round of PCR
VL2-rev	TGACTGGAGTTCAGACGTGTGCTCTTCCGATCTNNNNTNNNNTNNNNAGGACGGTCAGCTGGGTCCC	First round of PCR
VL3-rev	TGACTGGAGTTCAGACGTGTGCTCTTCCGATCTNNNNTNNNNTNNNNAGGACGGTCACCTTGGTGCC	First round of PCR
VL4-rev	TGACTGGAGTTCAGACGTGTGCTCTTCCGATCTNNNNTNNNNTNNNNAGGACGGTCAGCTGGGTGCC	First round of PCR
Illumida adaptor amp-fwd	AATGATACGGCGACCACCGAGATCTACAC [i5 index] ACACTCTTTCCCTACACGACGCTCTTCCGATC	Second round of PCR
Illumida adaptor amp-rev	CAAGCAGAAGACGGCATACGAGAT [i7 index] GTGACTGGAGTTCAGACGTGTGCTCTTCCG	Second round of PCR

Primers used for the amplification of V_H from the phage library

Name	Sequence	Step
VH-fwd	AATGATACGGCGACCACCGAGATCTACAC [8mer Index sequence] ACACTCTTTCCCTACACGACGCTCTTCCGATCT	V_H amplification for NGS
VH-rev	CAAGCAGAAGACGGCATACGAGAT [8mer Index sequence] GTGACTGGAGTTCAGACGTGTGCTCTTCCGATCT	V_H amplification for NGS

Primers used for the construction of human scFv libraries

Name	Sequence	Step
VL1-fwd	GGGCCCAGGCGGCCGAGCTCGTGCTGACTCAGCCACCC	First round of PCR
VL2-fwd	GGGCCCAGGCGGCCGAGCTCGTGCTGACGCAGCCGC	First round of PCR
VL3-fwd	GGGCCCAGGCGGCCGAGCTCGTCGTGACGCAGCCGC	First round of PCR
VL4-fwd	GGGCCCAGGCGGCCGAGCTCGTGTTGACGCAGCCGCC	First round of PCR
VL5-fwd	GGGCCCAGGCGGCCGAGCTCGGGCTGACTCAGCCACCC	First round of PCR
VL6-fwd	GGGCCCAGGCGGCCGAGCTCGCCCTGACTCAGCCTCGC	First round of PCR
VL7-fwd	GGGCCCAGGCGGCCGAGCTCGCCCTGACTCAGCCTGCC	First round of PCR
VL8-fwd	GGGCCCAGGCGGCCGAGCTCGCCCTGACTCAGCCTCCC	First round of PCR
VL9-fwd	GGGCCCAGGCGGCCGAGCTCGAGCTGACTCAGCCACCCTC	First round of PCR
VL10-fwd	GGGCCCAGGCGGCCGAGCTCGAGCTGACACAGCCACCCTC	First round of PCR
VL11-fwd	GGGCCCAGGCGGCCGAGCTCGAGCTGACTCAGCCACACTC	First round of PCR
VL12-fwd	GGGCCCAGGCGGCCGAGCTCGAGCTGACTCAGGACCCTGC	First round of PCR
VL13-fwd	GGGCCCAGGCGGCCGAGCTCGAGCTGACACAGCTACCCTCG	First round of PCR
VL14-fwd	GGGCCCAGGCGGCCGAGCTCGAGCTGATGCAGCCACCC	First round of PCR
VL15-fwd	GGGCCCAGGCGGCCGAGCTCGAGCTGACACAGCCATCCTCA	First round of PCR
VL16-fwd	GGGCCCAGGCGGCCGAGCTCGAGCTGACTCAGCCACTCTCA	First round of PCR
VL17-fwd	GGGCCCAGGCGGCCGAGCTCGTGCTGACTCAGCCCCCG	First round of PCR
VL18-fwd	GGGCCCAGGCGGCCGAGCTCGTGCTGACTCAATCATCCTCT	First round of PCR
VL19-fwd	GGGCCCAGGCGGCCGAGCTCGTGCTGACTCAATCGCCCTCT	First round of PCR
VL20-fwd	GGGCCCAGGCGGCCGAGCTCGTGCTGACTCAGCCACCTTC	First round of PCR
VL21-fwd	GGGCCCAGGCGGCCGAGCTCGTGCTGACTCAGCCAACCTC	First round of PCR
VL22-fwd	GGGCCCAGGCGGCCGAGCTCGTGCTGACTCAGCCGGCT	First round of PCR
VL23-fwd	GGGCCCAGGCGGCCGAGCTCGTGCTGACTCAGCCGTCTTC	First round of PCR
VL24-fwd	GGGCCCAGGCGGCCGAGCTCGTGCTGACTCAGCCATCTTCC	First round of PCR
VL25-fwd	GGGCCCAGGCGGCCGAGCTCATGCTGACTCAGCCCCACTC	First round of PCR
VL26-fwd	GGGCCCAGGCGGCCGAGCTCGTGGTGACTCAGGAGCCCTC	First round of PCR
VL27-fwd	GGGCCCAGGCGGCCGAGCTCGTGGTGACCCAGGAGCCATC	First round of PCR

VL1-rev	GGAAGATCTAGAGGAACCACCGCCTAGGACGGTGACCTTGGTCC	First round of PCR
VL2-rev	GGAAGATCTAGAGGAACCACCGCCTAGGACGGTCAGCTTGGTCC	First round of PCR
VL3-rev	GGAAGATCTAGAGGAACCACCGCCGAGGACGGTCACCTTGGTG	First round of PCR
VL4-rev	GGAAGATCTAGAGGAACCACCGCCGAGGACGGTCAGCTGGGTG	First round of PCR
VL5-rev	GGAAGATCTAGAGGAACCACCGCCGAGGGCGGTCAGCTGGG	First round of PCR
VK1-fwd	GGGCCCAGGCGGCCGAGCTCCAGATGACCCAGTCTCCATCT	First round of PCR
VK2-fwd	GGGCCCAGGCGGCCGAGCTCCAGTTGACCCAGTCTCCATCC	First round of PCR
VK3-fwd	GGGCCCAGGCGGCCGAGCTCCAGATGACCCAGTCTCCATCC	First round of PCR
VK4-fwd	GGGCCCAGGCGGCCGAGCTCCAGATGACCCAGTCTCCTTCC	First round of PCR
VK5-fwd	GGGCCCAGGCGGCCGAGCTCCGGATGACCCAGTCTCCATC	First round of PCR
VK6-fwd	GGGCCCAGGCGGCCGAGCTCCGGATGACCCAGTCTCCATTC	First round of PCR
VK7-fwd	GGGCCCAGGCGGCCGAGCTCTGGATGACCCAGTCTCCATCC	First round of PCR
VK8-fwd	GGGCCCAGGCGGCCGAGCTCGTGATGACCCAGACTCCACTC	First round of PCR
VK9-fwd	GGGCCCAGGCGGCCGAGCTCGTGATGACTCAGTCTCCACTC	First round of PCR
VK10-fwd	GGGCCCAGGCGGCCGAGCTCGTGTTGACACAGTCTCCAGC	First round of PCR
VK11-fwd	GGGCCCAGGCGGCCGAGCTCGTGATGACGCAGTCTCCAGC	First round of PCR
VK12-fwd	GGGCCCAGGCGGCCGAGCTCGTGTTGACGCAGTCTCCAG	First round of PCR
VK13-fwd	GGGCCCAGGCGGCCGAGCTCGTAATGACACAGTCTCCAGCC	First round of PCR
VK14-fwd	GGGCCCAGGCGGCCGAGCTCGTGATGACCCAGTCTCCAGAC	First round of PCR
VK15-fwd	GGGCCCAGGCGGCCGAGCTCACACTCACGCAGTCTCCAG	First round of PCR
VK16-fwd	GGGCCCAGGCGGCCGAGCTCGTGCTGACTCAGTCTCCAGAC	First round of PCR
VK-1-rev	GGAAGATCTAGAGGAACCACCTTTGATTTCCACCTTGGTCCC	First round of PCR
VK-2-rev	GGAAGATCTAGAGGAACCACCTTTGATCTCCAGCTTGGTCCC	First round of PCR
VK-3-rev	GGAAGATCTAGAGGAACCACCTTTGATATCCACTTTGGTCCC	First round of PCR
VK-4-rev	GGAAGATCTAGAGGAACCACCTTTGATCTCCACCTTGGTCCC	First round of PCR
VK-5-rev	GGAAGATCTAGAGGAACCACCTTTAATCTCCAGTCGTGTCCC	First round of PCR
VH1-fwd	GGTGGTTCCTCTAGATCTTCCTCCTCTGGTGGCGGTGGCTCGGGCGGTGGTGGGCAGGTTCAGCTGGTGCAGTC	First round of PCR
VH2-fwd	GGTGGTTCCTCTAGATCTTCCTCCTCTGGTGGCGGTGGCTCGGGCGGTGGTGGGCAGGTGCAGCTGGTGCAG	First round of PCR
VH3-fwd	GGTGGTTCCTCTAGATCTTCCTCCTCTGGTGGCGGTGGCTCGGGCGGTGGTGGGCAGGTCCAGCTGGTACAGTCT	First round of PCR
VH4-fwd	GGTGGTTCCTCTAGATCTTCCTCCTCTGGTGGCGGTGGCTCGGGCGGTGGTGGGCAGGTCCAGCTTGTGCAGTC	First round of PCR
VH5-fwd	GGTGGTTCCTCTAGATCTTCCTCCTCTGGTGGCGGTGGCTCGGGCGGTGGTGGGCAGATGCAGCTGGTGCAGTC	First round of PCR
VH6-fwd	GGTGGTTCCTCTAGATCTTCCTCCTCTGGTGGCGGTGGCTCGGGCGGTGGTGGGCAAATGCAGCTGGTGCAGTC	First round of PCR
VH7-fwd	GGTGGTTCCTCTAGATCTTCCTCCTCTGGTGGCGGTGGCTCGGGCGGTGGTGGGCAGGTCCAGCTGGTGCAATC	First round of PCR
VH8-fwd	GGTGGTTCCTCTAGATCTTCCTCCTCTGGTGGCGGTGGCTCGGGCGGTGGTGGGCAGGTCCAGCTGGTGCAG	First round of PCR
VH9-fwd	GGTGGTTCCTCTAGATCTTCCTCCTCTGGTGGCGGTGGCTCGGGCGGTGGTGGGGAGGTCCAGCTGGTACAGTC	First round of PCR
VH10-fwd	GGTGGTTCCTCTAGATCTTCCTCCTCTGGTGGCGGTGGCTCGGGCGGTGGTGGGCAGGTCACCTTGAAGGAGTCT	First round of PCR
VH11-fwd	GGTGGTTCCTCTAGATCTTCCTCCTCTGGTGGCGGTGGCTCGGGCGGTGGTGGGCAGATCACCTTGAAGGAGTCT	First round of PCR
VH12-fwd	GGTGGTTCCTCTAGATCTTCCTCCTCTGGTGGCGGTGGCTCGGGCGGTGGTGGGCAGGTCACCTTGAGGGAGTC	First round of PCR
VH13-fwd	GGTGGTTCCTCTAGATCTTCCTCCTCTGGTGGCGGTGGCTCGGGCGGTGGTGGGCGGGTCACCTTGAGGGAG	First round of PCR
VH14-fwd	GGTGGTTCCTCTAGATCTTCCTCCTCTGGTGGCGGTGGCTCGGGCGGTGGTGGGCAGGTGCAGCTGGTGGAG	First round of PCR
VH15-fwd	GGTGGTTCCTCTAGATCTTCCTCCTCTGGTGGCGGTGGCTCGGGCGGTGGTGGGCAGGTGCAGCTGTTGGAGTC	First round of PCR
VH16-fwd	GGTGGTTCCTCTAGATCTTCCTCCTCTGGTGGCGGTGGCTCGGGCGGTGGTGGGGAGGTGCAGCTGGTGGAG	First round of PCR
VH17-fwd	GGTGGTTCCTCTAGATCTTCCTCCTCTGGTGGCGGTGGCTCGGGCGGTGGTGGGGAGGTGCATCTGGTGGAGTC	First round of PCR
VH18-fwd	GGTGGTTCCTCTAGATCTTCCTCCTCTGGTGGCGGTGGCTCGGGCGGTGGTGGGGAGGTGCAACTGGTGGAGTC	First round of PCR
VH19-fwd	GGTGGTTCCTCTAGATCTTCCTCCTCTGGTGGCGGTGGCTCGGGCGGTGGTGGGGAGGTGCAGCTGTTGGAGTC	First round of PCR
VH20-fwd	GGTGGTTCCTCTAGATCTTCCTCCTCTGGTGGCGGTGGCTCGGGCGGTGGTGGGCAGGTGCAGCTGGTGGAC	First round of PCR
VH21-fwd	GGTGGTTCCTCTAGATCTTCCTCCTCTGGTGGCGGTGGCTCGGGCGGTGGTGGGCAGGTACAGCTGGTGGAGTC	First round of PCR
VH22-fwd	GGTGGTTCCTCTAGATCTTCCTCCTCTGGTGGCGGTGGCTCGGGCGGTGGTGGGGAAGTGCAGCTGGTGGAGTC	First round of PCR
VH23-fwd	GGTGGTTCCTCTAGATCTTCCTCCTCTGGTGGCGGTGGCTCGGGCGGTGGTGGGCAGGTGCAGCTGCAGGAG	First round of PCR
VH24-fwd	GGTGGTTCCTCTAGATCTTCCTCCTCTGGTGGCGGTGGCTCGGGCGGTGGTGGGCAGGTGCAGCTACAGGAGTC	First round of PCR
VH25-fwd	GGTGGTTCCTCTAGATCTTCCTCCTCTGGTGGCGGTGGCTCGGGCGGTGGTGGGCAGGTACAGCTGCAGGAGTC	First round of PCR
VH26-fwd	GGTGGTTCCTCTAGATCTTCCTCCTCTGGTGGCGGTGGCTCGGGCGGTGGTGGGCAGCTGCAGCTGCAGGAG	First round of PCR
VH27-fwd	GGTGGTTCCTCTAGATCTTCCTCCTCTGGTGGCGGTGGCTCGGGCGGTGGTGGGCAGGTGCAGCTACAGCAGTG	First round of PCR
VH28-fwd	GGTGGTTCCTCTAGATCTTCCTCCTCTGGTGGCGGTGGCTCGGGCGGTGGTGGGCAGGTGCAGCTACAACAGTGG	First round of PCR
VH29-fwd	GGTGGTTCCTCTAGATCTTCCTCCTCTGGTGGCGGTGGCTCGGGCGGTGGTGGGCGGCTGCAGCTGCAGG	First round of PCR
VH30-fwd	GGTGGTTCCTCTAGATCTTCCTCCTCTGGTGGCGGTGGCTCGGGCGGTGGTGGGGAAGTGCAGCTGGTGCAGTC	First round of PCR
VH31-fwd	GGTGGTTCCTCTAGATCTTCCTCCTCTGGTGGCGGTGGCTCGGGCGGTGGTGGGGAGGTGCAGCTGGTGCAG	First round of PCR
VH32-fwd	GGTGGTTCCTCTAGATCTTCCTCCTCTGGTGGCGGTGGCTCGGGCGGTGGTGGGCAGGTACAGCTGCAGCAGTC	First round of PCR
VH33-fwd	GGTGGTTCCTCTAGATCTTCCTCCTCTGGTGGCGGTGGCTCGGGCGGTGGTGGGCAGGTGCAGCTGGTGCAATC	First round of PCR
VH1-rev	CCTGGCCGGCCTGGCCACTAGTTGAGGAGACGGTGACCAGG	First round of PCR
VH2-rev	CCTGGCCGGCCTGGCCACTAGTTGAGGAGACAGTGACCAGGG	First round of PCR
VH3-rev	CCTGGCCGGCCTGGCCACTAGTTGAAGAGACGGTGACCATTGT	First round of PCR
VH4-rev	CCTGGCCGGCCTGGCCACTAGTTGAGGAGACGGTGACCGTG	First round of PCR
AMP-VH-fwd	GGTGGTTCCTCTAGATCTTCCTCC	Second round of PCR
AMP-VH-rev	CCTGGCCGGCCTGGCCAC	Second round of PCR
AMP-K/L-fwd	GGGCCCAGGCGGCCGAG	Second round of PCR
AMP-K/L-rev	GGAAGATCTAGAGGAACCACC	Second round of PCR
EXT-fwd	GAGGAGGAGGAGGAGGAGGCGGGGCCCAGGCGGCCGAGCTC	Overlap extension
EXT-rev	GAGGAGGAGGAGGAGGAGCCTGGCCGGCCTGGCCACTAGT	Overlap extension

Primers used for the generation of RBD mutants

Name	Sequence	Step
RBD-fwd	GGCCCAGGCGGCCTTTACA	First and second round of PCR
RBD-rev	GGCCGGCCTGGCCAAAGTTG	First and second round of PCR
N354D-fwd	GTGTCTACGCATGGGACAGAAAGAGAATCAGT	First round of PCR
N354D-rev	ACTGATTCTCTTTCTGTCCCATGCGTAGACAC	First round of PCR
D364Y-fwd	GTAACTGTGTAGCGTACTATAGTGTCCTTTAT	First round of PCR
D364Y-rev	ATAAAGGACACTATAGTACGCTACACAGTTAC	First round of PCR
V367F-fwd	TGTGTAGCGGATTATAGTTTCCTTTATAATTCAGC	First round of PCR
V367F-rev	GCTGAATTATAAAGGAAACTATAATCCGCTACACA	First round of PCR
F342L-fwd	TTCGGGGAAGTGCTGAACGCTACCCG	First round of PCR
F342L-rev	CGGGTAGCGTTCAGCACTTCCCCGAA	First round of PCR
R408I-fwd	GAGATGAGGTGATTCAAATCGCGC	First round of PCR
R408I-rev	GCGCGATTTGAATCACCTCATCTC	First round of PCR
W436R-fwd	GGATGTGTTATCGCTAGAAACTCTAACAAC	First round of PCR
W436R-rev	GTTGTTAGAGTTTCTAGCGATAACACATCC	First round of PCR
V341I-fwd	CATTCGGGGAAATCTTTAACGCTACC	First round of PCR
V341I-rev	GGTAGCGTTAAAGATTTCCCCGAATG	First round of PCR
A435S-fwd	GGGATGTGTTATCAGCTGGAACTCTAAC	First round of PCR
A435S-rev	GTTAGAGTTCCAGCTGATAACACATCCC	First round of PCR

G476S-fwd	ATTTATCAGGCTAGCAGCACACCTTG	First round of PCR
G476S-rev	CAAGGTGTGCTGCTAGCCTGATAAAT	First round of PCR
V483A-fwd	CACCTTGCAATGGTGCCGAAGGATTCAA	First round of PCR
V483A-rev	TTGAATCCTTCGGCACCATTGCAAGGTG	First round of PCR